



Deimination Protein Profiles in Alligator mississippiensis Reveal Plasma and Extracellular Vesicle-Specific Signatures Relating to Immunity, Metabolic Function, and Gene Regulation

Michael F. Criscitiello 1,2, Igor Kraev 3, Lene H. Petersen 4 and Sigrun Lange 5*

¹ Comparative Immunogenetics Laboratory, Department of Veterinary Pathobiology, College of Veterinary Medicine and Biomedical Sciences, Texas A&M University, College Station, TX, United States, ² Department of Microbial Pathogenesis and Immunology, College of Medicine, Texas A&M Health Science Center, Texas A&M University, College Station, TX, United States, ³ Electron Microscopy Suite, Faculty of Science, Technology, Engineering and Mathematics, Open University, Milton Keynes, United Kingdom, ⁴ Department of Marine Biology, Texas A&M University at Galvestone, Galveston, TX, United States, ⁵ Tissue Architecture and Regeneration Research Group, School of Life Sciences, University of Westminster, London, United Kingdom

OPEN ACCESS

Edited by:

Fabrizio Ceciliani, University of Milan, Italy

Reviewed by:

Marie-Claire Mechin, Université Toulouse III Paul Sabatier, France Hai-peng Liu, Xiamen University, China

*Correspondence:

Sigrun Lange s.lange@westminster.ac.uk

Specialty section:

This article was submitted to Comparative Immunology, a section of the journal Frontiers in Immunology

Received: 04 February 2020 Accepted: 23 March 2020 Published: 28 April 2020

Citation:

Criscitiello MF, Kraev I, Petersen LH and Lange S (2020) Deimination Protein Profiles in Alligator mississippiensis Reveal Plasma and Extracellular Vesicle-Specific Signatures Relating to Immunity, Metabolic Function, and Gene Regulation. Front. Immunol. 11:651. doi: 10.3389/fimmu.2020.00651

Alligators crocodilians and among few species that endured the Cretaceous-Paleogene extinction event. With long life spans, low metabolic rates, unusual immunological characteristics, including strong antibacterial and antiviral ability, and cancer resistance, crocodilians may hold information for molecular pathways underlying such physiological traits. Peptidylarginine deiminases (PADs) are a group of calcium-activated enzymes that cause posttranslational protein deimination/citrullination in a range of target proteins contributing to protein moonlighting functions in health and disease. PADs are phylogenetically conserved and are also a key regulator of extracellular vesicle (EV) release, a critical part of cellular communication. As little is known about PAD-mediated mechanisms in reptile immunology, this study was aimed at profiling EVs and protein deimination in Alligator mississippiensis. Alligator plasma EVs were found to be polydispersed in a 50-400-nm size range. Key immune, metabolic, and gene regulatory proteins were identified to be posttranslationally deiminated in plasma and plasma EVs, with some overlapping hits, while some were unique to either plasma or plasma EVs. In whole plasma, 112 target proteins were identified to be deiminated, while 77 proteins were found as deiminated protein hits in plasma EVs, whereof 31 were specific for EVs only, including proteins specific for gene regulatory functions (e.g., histones). Gene Ontology (GO) and Kyoto Encyclopedia of Genes and Genomes (KEGG) enrichment analysis revealed KEGG pathways specific to deiminated proteins in whole plasma related to adipocytokine signaling, while KEGG pathways of deiminated proteins specific to EVs included ribosome, biosynthesis of amino acids, and glycolysis/gluconeogenesis pathways as well as core histones. This highlights roles for EV-mediated export of deiminated protein cargo with roles in metabolism and gene regulation, also related to cancer. The identification of posttranslational deimination and EV-mediated communication

1

in alligator plasma revealed here contributes to current understanding of protein moonlighting functions and EV-mediated communication in these ancient reptiles, providing novel insight into their unusual immune systems and physiological traits. In addition, our findings may shed light on pathways underlying cancer resistance, antibacterial and antiviral resistance, with translatable value to human pathologies.

Keywords: peptidylarginine deiminases, protein deimination/citrullination, American alligator (Alligator mississippiensis), extracellular vesicles, immunity, metabolism, antimicrobial/antiviral

INTRODUCTION

Alligators are crocodilians, with two living species, the American alligator (Alligator mississippiensis) and the Chinese alligator (Alligator sinensis). Alligators are long-lived ancient animals and, alongside crocodiles, are among the few species who endured the Cretaceous-Paleogene extinction event. Crocodilians appeared ~240 million years ago, during the Middle Triassic. Although crocodilians are similar in appearance to other reptiles, they are only distantly related to lizards and belong to the closest extant relatives of birds, therefore occupying an important evolutionary position (1-3). Alligators can endure and occupy unsanitary environments, withstand radiation of high levels, and be routinely exposed to heavy metals but are rarely reported to develop cancer (4). With long life spans and unusual immunological characteristics, including unique antimicrobial responses (5-8), antiviral activity against enveloped viruses, including HIV (9) and low metabolic rate (10), crocodilians may hold information for molecular pathways underlying such unusual physiological traits.

Peptidylarginine deiminases (PADs) are a group of calcium-dependent enzymes that posttranslationally convert arginine into citrulline in target proteins in an irreversible manner (11). Such calcium-mediated deimination/citrullination can lead to structural and sometimes functional changes in target proteins and therefore affect protein function (12, 13). A range of proteins known to undergo this posttranslational modification belong to cytoplasmic, nuclear, and mitochondrial targets, and therefore, depending on which target proteins are modified, deimination can for example contribute to the generation of neo-epitopes as well as affecting gene regulation (14–22). Such posttranslational changes in proteins may also allow for protein moonlighting, an evolutionarily acquired phenomenon facilitating proteins to exhibit several physiologically relevant functions within one polypeptide chain (23, 24).

PADs and associated protein deimination are crucial players in cancer and autoimmune and neurodegenerative diseases (17, 19, 20, 22, 25). PADs have received particular attention due to roles in cancer (20, 22, 26, 27), rheumatoid arthritis (28–33), multiple sclerosis (34–38), as well as due to their contribution to skin physiology and diseases (39). PADs have furthermore been shown to play crucial roles in hypoxia and CNS regeneration (40–44), and roles for PAD2 in promotion of oligodendrocyte differentiation and myelination have been shown (45). PAD-mediated mechanisms have also been related to aging (46, 47). Importantly, PADs have also been implicated

in infection, including sepsis and endotoxemia (48–55). Roles for PADs in tissue remodeling and immunity have also recently been described (56–58). PADs have furthermore been identified as important regulators of the release of extracellular vesicles (EVs) (27, 59–62). EVs participate in cellular communication via transfer of cargo proteins and genetic material and can be isolated from most body fluids (20, 63–66). As EV cargo is comprised of a large range of proteins, enzymes, and genetic material, characteristic of the cells of origin, EV signatures can be useful biomarkers and easily isolated from a range of body fluids, including serum and plasma (67, 68). While work on EVs has largely focused on human pathologies, an increasing body of comparative studies with respect to EVs and EV cargo has been performed in a range of taxa, including by our group (69–80).

PADs have been identified in diverse taxa throughout phylogeny, from bacteria to mammals. In mammals, five tissue-specific PAD isozymes with deimination activity are described: three in chicken, one in bony and cartilaginous fish (14, 56, 58, 76, 81), and PAD homologs (arginine deiminases, ADI) in parasites (82), fungi (83), and bacteria (62, 84). While in the American alligator three PADI genes have been reported (PADI1, Gene ID: 102574884, Protein ID: XP_019355592.1; PADI2, Gene ID: 102574651, Protein ID: XP_019457295.1), no studies have hitherto been carried out on PAD protein function and putative physiological relevance for PAD-mediated posttranslational deimination in crocodilians.

Plasma of the American alligator has previously been evaluated for its exceptional antibacterial activity, including a cathelicidin, which has been identified to show promise against multidrug-resistant *Acinetobacter* without toxicity to eukaryotic cells (8). Blood and plasma biochemistry for baseline physiology assessment has been carried out in alligator (85) as well as corticosterone characterization for assessment of environmental stressors (86), including chronic exposure to selenium (87). To date though, no assessment of EVs has been carried out in crocodilians, and therefore, the roles for EVs in the unusual immune responses and metabolism of alligators remain to be further explored and may provide novel biomarkers.

This current study profiled plasma and plasma-derived EVs for deiminated protein signatures in the American alligator. For the first time, this posttranslational modification is assessed in crocodilians, reporting deimination of key immune, metabolic, and nuclear proteins in alligator and species-specific EV signatures. Our findings provide novel insight into the

unusual physiology of crocodilians and may further current understanding of pathways underlying cancer, antiviral and antibacterial resistance.

MATERIALS AND METHODS

Plasma Sampling From Alligator

Blood was collected from the occipital sinus of three healthy young male alligators (weight, 2,538, 2,850, and 2,810 g; snoutvent length, 42.1, 47.1, and 47.2 cm, respectively), and plasma was prepared as previously described (88). In brief, blood samples were collected from the occipital sinus, quickly placed in a nonheparinized microfuge tube, and immediately centrifuged for 2 min at 10,000 g to separate the plasma (88). Sample collection was conducted under Texas A&M Institutional Animal Care and Use Protocol # 2015-0347. Plasma was aliquoted and kept at $-80^{\circ}\mathrm{C}$ until used.

Isolation of Extracellular Vesicles and Nanoparticle Tracking Analysis (NTA)

Plasma aliquots that had been collected as described above and kept frozen at -80°C were thawed. Plasma EVs were isolated from plasma of individual animals (n = 3), using sequential centrifugation and ultracentrifugation in accordance with previously established protocols (61, 76, 79) and according to the recommendations of the minimal information for studies of extracellular vesicles 2018 [MISEV2018; (89)]. For each individual EV preparation, 100 µl of alligator plasma were diluted 1:5 in Dulbecco's phosphate-buffered saline (DPBS, ultrafiltered using a 0.22-µm filter, before use) and then centrifuged at 4,000 g for 30 min at 4°C, to ensure the removal of aggregates and apoptotic bodies. Thereafter, the supernatants were collected and centrifuged further, using ultracentrifugation at 100,000 g for 1 h at 4°C. The EV-enriched pellets were resuspended in 1 ml DPBS and ultracentrifuged again at 100,000 g for 1 h at 4°C. The resulting washed EV pellets were then resuspended in 100 μl DPBS and frozen at -80°C until further use. For EV size distribution profiles and EV quantification, nanoparticle tracking analysis (NTA) was carried out using the NanoSight NS300 system (Malvern, UK), which analyzes particle size based on Brownian motion. The EV samples were diluted 1/100 in DPBS (10 µl of EV preparation diluted in 990 µl of DPBS) and applied to the NanoSight using a syringe pump to ensure continuous flow of the sample. For each sample, five 60-s videos were recorded, keeping the number of particles per frame in between 40 and 60. Replicate histograms were generated from the videos, using the NanoSight software 3.0 (Malvern), representing mean and confidence intervals of the five recordings for each sample.

Transmission Electron Microscopy

A pool of EVs, isolated from plasma of the three individual animals as described above, was used for morphological analysis using transmission electron microscopy (TEM), according to previously described methods (79, 80). Following isolation, the EVs were frozen at -80° C and used within 3 days for TEM imaging. Before TEM preparation, the EVs were thawed and

resuspended in 100 mM sodium cacodylate buffer (pH 7.4), and a drop (\sim 3-5 μ l) of the suspension was placed onto a grid with previously glow-discharged carbon support film. After the suspension had partly dried, the EVs were fixed by placing the grid onto a drop of a fixative solution [2.5% glutaraldehyde in 100 mM sodium cacodylate buffer (pH 7.0)] for 1 min at room temperature and washed afterwards by touching the grid to the surface of three drops of distilled water. Excess water was removed by touching the grid to a filter paper. Next, the EVs were stained with 2% aqueous uranyl acetate (Sigma-Aldrich) for 1 min, the excess stain was removed by touching the grid edge to a filter paper, and the grid was let to dry. Imaging of EVs was performed using a JEOL JEM 1400 transmission electron microscope (JEOL, Japan) operated at 80 kV at a magnification of 30,000-60,000×. Digital images were recorded using an AMT XR60 CCD camera (Deben, UK).

Isolation of Deiminated Proteins Using F95 Enrichment

Immunoprecipitation and isolation of deiminated proteins in plasma and plasma-derived EVs was carried out as previously described (76), using the Catch and Release® v2.0 immunoprecipitation kit (Merck, UK) in conjunction with the F95 pan-deimination antibody (MABN328, Merck), which has been developed against a deca-citrullinated peptide and specifically detects proteins modified by deimination/citrullination (90). Alligator plasma pools of the three individual animals (3 \times 25 μ l) were used for F95 enrichment from whole plasma, while for EVs, total protein was first extracted from a pool of EVs derived from three animals (EV pellets derived from 100 µl plasma per animal), using RIPA+ buffer (Sigma, UK). Following application of RIPA+ buffer, the EVs were incubated on ice for 2h followed by centrifugation at 16,000 g for 30 min to collect the protein containing supernatant. Thereafter, immunoprecipitation (F95 enrichment) was carried out overnight on a rotating platform at 4°C. F95-enriched proteins were eluted according to the manufacturer's instructions (Merck), using denaturing elution buffer (Merck), and diluted 1:1 in Laemmli sample buffer. The F95-enriched eluates from whole plasma and plasma-EVs were then analyzed by sodium dodecyl sulfate-polyacrylamide gel electrophoresis (SDS-PAGE), followed by Western blotting, silver staining, or liquid chromatography with tandem mass spectrometry (LC-MS/MS).

Western Blotting Analysis

Alligator plasma and plasma EVs were diluted 1:1 in denaturing 2× Laemmli sample buffer (containing 5% beta-mercaptoethanol, BioRad, UK) and boiled for 5 min at 100°C. Proteins were separated by SDS-PAGE using 4–20% gradient TGX gels (BioRad, UK). Western blotting was carried out using the Trans-Blot® SD semidry transfer cell (BioRad, UK); even transfer was assessed by staining the membranes with PonceauS (Sigma, UK). Blocking was performed for 1 h at room temperature using 5% bovine serum albumin (BSA, Sigma, UK), in Tris-buffered saline (TBS) containing 0.1% Tween 20 (TBS-T; BioRad, UK). Following blocking, the

membranes were incubated overnight at 4°C on a shaking platform with the primary antibodies, which were diluted in TBS-T. For the detection of deiminated/citrullinated proteins, the F95 pan-deimination antibody was used (MABN328, Merck, 1/1,000). For the detection of putative PAD proteins in alligator plasma, cross-reaction with antihuman PAD2, PAD3, and PAD4 was assessed using the following antihuman PAD antibodies: anti-PAD2 (ab50257, Abcam, 1/1,000), anti-PAD3 (ab50246, Abcam, 1/1,000), and anti-PAD4 (ab50247, Abcam, 1/1,000), which have previously been shown to cross-react with PAD homologs in a range of taxa (40, 41, 56, 58, 76, 77, 79, 80). Crossreaction with antibodies against other human PAD isozymes was not assessed in the current study (PAD1 or PAD6). For the detection of deiminated histone H3, the citH3 antibody was used (citH3, Abcam, 1/1,000), which is also a marker of neutrophil extracellular trap formation (NETosis). EV isolates were blotted against two EV-specific markers: CD63 (ab216130, 1/1,000) and Flotillin-1 (Flot-1, ab41927, ½,000), for the characterization of EVs. After primary antibody incubation, the membranes were washed for 3× 10 min in TBS-T at room temperature (RT) and incubated for 1 h, at RT with horseradish peroxidase (HRP)conjugated secondary antibodies [antirabbit immunoglobulin G (IgG) (BioRad) or antimouse IgM (BioRad) respectively, diluted 1/3,000 in TBS-T]. The membranes were then washed in TBS-T for 5× 10 min, and positive proteins bands were visualized digitally, using enhanced chemiluminescence (ECL; Amersham, UK) and the UVP BioDoc-ITTM System (Thermo Fisher Scientific, UK).

Silver Staining

F95-enriched protein eluates from alligator plasma and plasma EVs were silver stained following SDS-PAGE (4–20% gradient TGX gels, BioRad, UK) under reducing conditions. The BioRad Silver Stain Plus Kit (1610449, BioRad, UK) was used, according to the manufacturer's instructions (BioRad) and previously described methods (91).

Liquid Chromatography With Tandem Mass Spectrometry Analysis of Deiminated Protein Candidates

F95-enriched eluates from alligator plasma and plasma EVs were analyzed by LC-MS/MS as previously described (79, 80). For LC-MS/MS analysis, the F95-enriched eluates were run 0.5 cm into a 12% TGX gel (BioRad, UK), the band cut out, trypsin digested, and subjected to proteomic analysis using a Dionex Ultimate 3000 RSLC nano-UPLC (Thermo Fisher Scientific Inc., Waltham, MA, USA) system and a QExactive Orbitrap mass spectrometer (Thermo Fisher Scientific Inc., Waltham, MA, USA). Peptides were separated by reverse-phase chromatography (flowrate, 300 nl/min) and using a Thermo Scientific reversephase nano Easy-Spray column (Thermo Scientific PepMap C18, $2 \mu m$ particle size, 100 A pore size, $75 \mu m$ i.d. \times 50 cm length). Peptides were next loaded onto a precolumn (Thermo Scientific PepMap 100 C18, 5 µm particle size, 100 A pore size, $300\,\mu\text{m}$ i.d. \times 5 mm length) for 3 min, from the Ultimate 3000 autosampler, in the presence of 0.1% formic acid, at a 10 µl/min flowrate. Thereafter, elution of peptides from the precolumn onto the analytical column was facilitated by switching the column valve (solvent A = water + 0.1% formic acid; solvent B = 80% acetonitrile, 20% water + 0.1% formic acid). A linear gradient of 2-40% B was employed for 30 min. The LC eluent was sprayed into the mass spectrometer (using the Easy-Spray source, Thermo Fisher Scientific Inc.). Measuring of all m/z values for eluting ions was performed using an Orbitrap mass analyzer; setting was at a resolution of 70,000 and scanning between m/z 380–1,500. For automatic isolation and generation of fragment ions by higher energy collisional dissociation (HCD, NCE, 25%), data-dependent scans (Top 20) were employed, in the HCD collision cell. The measurement of resulting fragment ions was then performed using the Orbitrap analyzer, which was set at a resolution of 17,500. Ions with unassigned charge states and singly charged ions were excluded from being selected for MS/MS. Furthermore, a dynamic exclusion window of 20 s was employed. The data were processed postrun, using Protein Discoverer (version 2.1., Thermo Scientific); all MS/MS data were converted to mgf files. For the identification of deiminated protein hits, the files were next submitted to Mascot (Matrix Science, London, UK) and searched against the UniProt Alligator mississippiensis_20191104 database (31974 sequences; 16476323 residues) and a common contaminant sequences (123 sequences; 40594 residues). The fragment mass and peptide tolerances were, respectively, set to 20 ppm and 0.1 Da. The significance threshold was set at p < 0.05, and the peptide cutoff score was set at 20 (analysis carried out by Cambridge Proteomics, Cambridge, UK).

Protein-Protein Interaction Network Analysis

For the identification and prediction of putative interaction networks for deiminated proteins identified in alligator plasma and plasma EVs, the Search Tool for the Retrieval of Interacting Genes/Proteins analysis (STRING; https://string-db.org/) was used as previously described (80). Protein networks were built based on the protein IDs and using the function of "search multiple proteins" in STRING, choosing "Alligator mississippiensis" as the species database. Settings for the analysis were set at "basic," and confidence was applied at "medium." Color lines connecting the nodes indicate the following evidence-based interactions for network edges: known interactions (based on curated databases, experimentally determined), coexpression or protein homology, predicted interactions (based on gene neighborhood, gene fusion, gene co-occurrence), or via text mining.

Phylogenetic Comparison of American Alligator PADs With Human PADs

Previously reported predicted alligator (*A. mississippiensis*) protein sequences for PAD1 (XP_006259278.3), PAD2 (XP_019355592.1), and PAD3 (XP_014457295.1) isozymes were aligned with human PAD isozyme sequences PAD1 (NP_037490.2), PAD2 (NP_031391.2), PAD3 (NP_057317.2), PAD4 (NP_036519.2), and PAD6 (NP_997304.3), using

Clustal Omega (https://www.ebi.ac.uk/Tools/msa/clustalo/). A neighbor-joining phylogeny tree was constructed.

Statistical Analysis

The histograms and the graphs were prepared using the Nanosight 3.0 software (Malvern, UK) and GraphPad Prism version 7 (GraphPad Software, San Diego, USA). NTA curves represent mean and standard error of mean (SEM), indicated by confidence intervals. STRING analysis (https://string-db.org/) was used for the prediction of protein–protein interaction networks. Significance was set at $p \leq 0.05$.

RESULTS

Characterization of Alligator Plasma EVs

Plasma EVs were assessed by nanoparticle tracking analysis (NTA) for particle numbers and size distribution using the NanoSight NS300 system, revealing a poly-dispersed population

of EVs in the size range of mainly 50–400 nm, albeit with some individual variation in EV profiles within these size ranges and peaks at smaller (30 nm) and larger (500 nm) sizes (Figure 1A). Further characterization of the EVs was performed by Western blotting using the EV-specific markers CD63 and Flot-1 (Figure 1B), and by TEM, confirming typical EV morphology (Figure 1C). Some variation was observed between the three individuals with respect to EV yield (Figure 1D) and modal EV size, which fell in the range of 110–170 nm (Figure 1E).

PAD Protein Homologs and Deiminated Proteins in Alligator Plasma and Plasma EVs

For assessment of alligator PAD protein homologs, antihuman PAD-isozyme-specific antibodies were used for Western blotting, identifying positive protein bands at an expected ~70–75 kDa size for cross-reaction with antihuman PAD2, PAD3, and PAD4

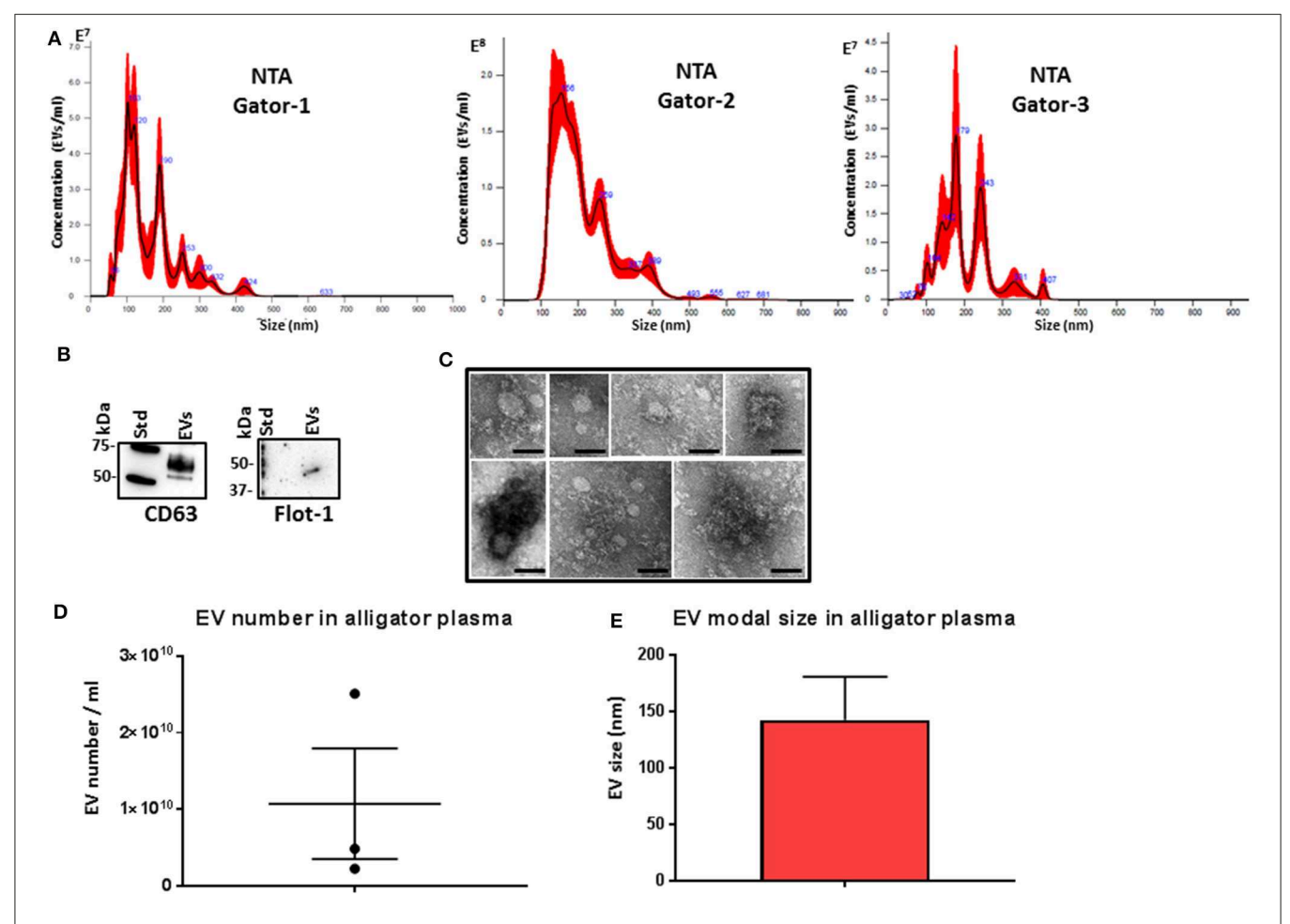


FIGURE 1 Extracellular vesicle profiling in alligator plasma. **(A)** Nanoparticle tracking analysis shows a size distribution of plasma extracellular vesicles (EVs) from *Alligator mississippiensis* in the size range of mainly 50–400 nm, albeit with some individual variation in EV profiles within these size ranges and peaks at smaller (30 nm) and larger (500 nm) sizes, with main peaks at \sim 50, 100, 200, 300, and 400 nm. **(B)** Western blotting analysis confirms that alligator EVs are positive for the phylogenetically conserved EV-specific markers CD63 and Flot-1. **(C)** Transmission electron microscopy (TEM) analysis of alligator plasma-derived EVs shows typical EV morphology; scale bar is 100 nm in all figures. **(D)** EV yield in alligator plasma (n = 3). **(E)** EV modal size in alligator plasma (n = 3).

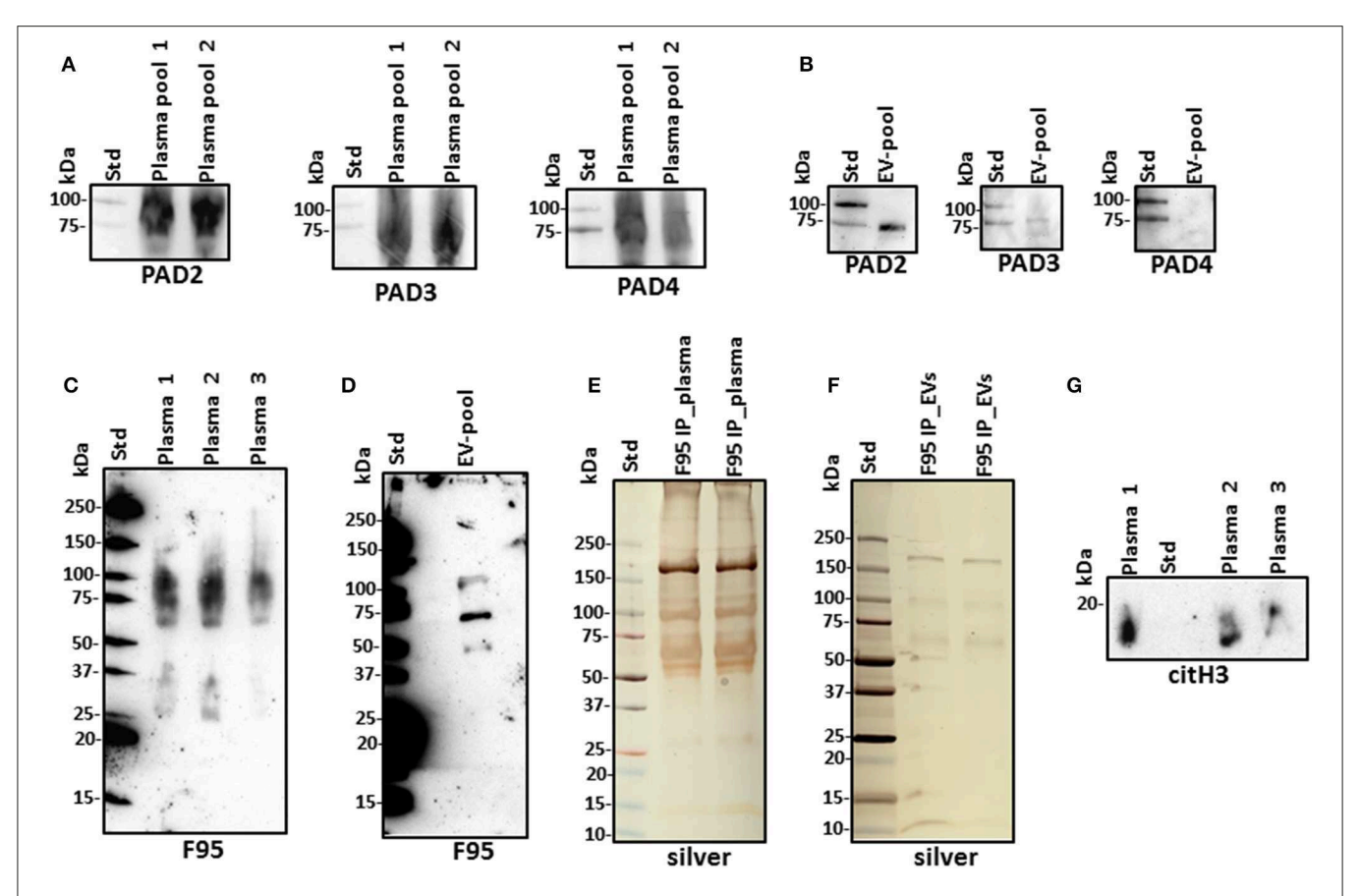


FIGURE 2 | Peptidylarginine deiminases (PADs) and deiminated proteins in alligator plasma and plasma extracellular vesicles (EVs). (A) PAD positive bands were identified at the expected size range of approximately 70–75 kDa using the antihuman PAD2-, PAD3-, and PAD4-specific antibodies in alligator plasma. (B) Plasma EVs show positive for PAD2 and for PAD3 at lower levels but negative for PAD4 (at expected 70–75 kDa size range), using antihuman PAD isozyme-specific antibodies against PAD2, PAD3, and PAD4, respectively. (C) Total deiminated proteins were identified in alligator plasma using the pan-deimination-specific F95 antibody. (D) Total deiminated proteins were identified in alligator plasma EVs using the pan-deimination-specific F95 antibody. (E,F) F95-enriched IP fraction from alligator plasma (E) and plasma EVs (F), shown by silver staining. (G) Deiminated histone H3 (citH3) is detected in alligator plasma. The F95-enriched IP fraction derived from a pool of three individual alligator plasma and a pool of plasma EVs (n = 3) is shown, respectively.

antibodies in plasma, although this was most prominent for anti-PAD2 (Figure 2A). In plasma EVs, cross-reaction with antihuman PAD2 antibody was prominent, and cross-reaction with antihuman PAD3 was detected at low levels, while the EVs did not show positive against the anti-human PAD4 antibody (Figure 2B). Cross-reaction with other antihuman PAD antibodies (against PAD1 or PAD6) was not tested in the current study. For assessment of total deiminated proteins present in plasma and plasma EVs, the pan-deimination F95 antibody revealed positive bands between 25 and 250 kDa in plasma (Figure 2C) and in EVs mainly in the size range of 50-150 kDa (Figure 2D). The F95-enriched fractions obtained by immunoprecipitation from alligator plasma and plasma EVs were assessed by SDS-PAGE and silver staining, showing protein bands in the size range of 15-250 kDa in plasma and 10-250 kDa in EVs (Figures 2E,F). The presence of deiminated histone H3, also a putative marker of NETosis, was confirmed in alligator plasma in the expected 17-20 kDa size range (Figure 2G).

LC-MS/MS Analysis of Deiminated Proteins in Alligator Plasma and Plasma EVs

Protein identification of deiminated proteins in alligator plasma and plasma EVs was carried out using F95 enrichment and LC-MS/MS analysis, searching for species-specific protein hits using the *Alligator mississippiensis* protein database. In plasma, 112 species-specific deiminated protein hits were identified (and further 33 species-specific uncharacterized protein hits) (**Table 1** and **Supplementary Table 1**). In plasma EVs, 77 species-specific deiminated protein hits were identified (and further 23 species-specific uncharacterized protein hits) (**Table 2** and **Supplementary Table 2**). Of the hits identified, 59 proteins were specific for whole plasma only (and an additional 17 uncharacterized alligator protein hits) and 24 proteins for EVs only (with an additional 7 uncharacterized alligator protein hits), while 53 hits overlapped (with an additional 16 unidentified alligator hits) (**Figure 3**).

Deiminated proteins in alligator plasma were isolated by immunoprecipitation using the pan-deimination F95 antibody.

TABLE 1 Deiminated proteins in plasma of alligator (*Alligator mississippiensis*), as identified by F95 enrichment and liquid chromatography with tandem mass spectrometry (LC-MS/MS) analysis.

Protein name Symbol Sequences Total score (p < 0.05)Uncharacterized protein A0A151NL74_ALLMI 84 5,545 (complement C3) Uncharacterized protein A0A151NM44 ALLMI 64 4.001 (venom factor) Uncharacterized protein A0A151NFJ9 ALLMI 55 3,599 Uncharacterized protein A0A151MJS8_ALLMI 55 3.527 A0A151NDR9 ALLMI Uncharacterized protein 51 3,205 Serum albumin A0A151N5S7_ALLMI 45 2,909 A0A151N5S7_ALLMI Fibrinogen beta chain 37 2,603 Uncharacterized protein A0A151N583_ALLMI 38 2,432 33 Fibrinogen gamma chain A0A151PB79_ALLMI 2.280 Alpha-2-macroglobulin-like A0A151NFQ0_ALLMI 28 2,233 Plasminogen A0A151M2C0_ALLMI 36 2,185 A0A151M2C2_ALLMI Plasminogen 36 2,184 A0A151MZ64_ALLMI 31 Uncharacterized protein 2.150 Complement receptor type A0A151MS72 ALLMI 27 1,798 1-like Uncharacterized protein A0A151NDR1_ALLMI 25 1,797 A0A151MJZ7_ALLMI Melanotransferrin 27 1 766 Kininogen-1 A0A151M678_ALLMI 24 1,693 A0A151NGB2_ALLMI 23 Hemopexin 1.662 Plasma kallikrein isoform B A0A151PAG7_ALLMI 26 1,627 Complement C5 A0A151NUM2 ALLMI 22 1,426 A0A151NLW7_ALLMI 20 1,328 Uncharacterized protein Uncharacterized protein A0A151MYR7 ALLMI 19 1,304 Uncharacterized protein A0A151MYS3_ALLMI 16 1.191 Uncharacterized protein A0A151MJK7_ALLMI 19 1,183 Uncharacterized protein A0A151NAV0_ALLMI 19 1,181 Fetuin-B isoform B A0A151M7P5_ALLMI 20 1,164 Complement factor H A0A151NM72_ALLMI 17 1,054 IgGFc-binding protein-like A0A151MJC3_ALLMI 14 1,043 Vitamin D-binding protein A0A151N541_ALLMI 19 998 Carbonic anhydrase 6 A0A151N4K1_ALLMI 15 920 A0A151MYV2_ALLMI 12 911 Uncharacterized protein A0A151P5P7_ALLMI Uncharacterized protein 15 873 CD5 antigen-like A0A151PHB7_ALLMI 13 867 792 Antithrombin-III A0A151MIW1_ALLMI 13 Uncharacterized protein A0A151MYX2_ALLMI 10 752 Uncharacterized protein A0A151PB91_ALLMI 9 726 Ovoinhibitor A0A151MEG6_ALLMI 11 625 Coagulation factor XII A0A151NM16_ALLMI 610 8 Alpha-1-inhibitor 3-like A0A151M7F0_ALLMI 11 591 T-cell surface glycoprotein A0A151P975_ALLMI 6 567 CD8 beta chain Hemoglobin subunit alpha-A A0A151P678_ALLMI 9 538 Uncharacterized protein A0A151MYQ9 ALLMI 8 514 Ig lambda chain V-1 region A0A151P8L7_ALLMI 6 500 A0A151MZ31_ALLMI Uncharacterized protein 7 484 Heparin cofactor 2 isoform B A0A151MLS1_ALLMI 9 483 Glutathione peroxidase A0A151MUD9_ALLMI 8 480

TABLE 1 | Continued

TABLE 1 Continued			
Protein name	Symbol	Sequences	Total score $(p < 0.05)^{\dagger}$
Uncharacterized protein	A0A151MYZ1_ALLM	I 6	479
Inter-alpha-trypsin inhibitor heavy chain H2 isoform A	A0A151NPL6_ALLMI	8	459
Ficolin-3	A0A151NG70_ALLM	l 8	455
Hemoglobin subunit beta	A0A151PG12_ALLMI	7	450
Ig epsilon chain C region	A0A151MYW1_ALLN	11 7	439
Apolipoprotein E	A0A151N3F1_ALLMI		430
Complement factor I	A0A151MIQ2_ALLMI	7	424
Fibrinogen C-terminal domain-containing protein	A0A151MF51_ALLMI		420
TED_complement domain-containing protein	A0A151N5Z3_ALLMI		417
Complement C1q subcomponent subunit B	A0A151MZU2_ALLM	I 6	374
Alpha-1-antitrypsin	A0A151P8U9_ALLMI		367
Uncharacterized protein	A0A151M7P2_ALLM		351
Coagulation factor XIII B chain	A0A151NCL4_ALLM	5	333
Alpha-1-antitrypsin	A0A151P8P3_ALLMI	6	322
Alpha-2-antiplasmin	A0A151LY18_ALLMI	6	321
Fructose-bisphosphate aldolase	A0A151MLN4_ALLM	I 4	303
Basement membrane-specific heparan sulfate proteoglycan core protein	A0A151MTT0_ALLMI	5	299
Coagulation factor XIII A chain isoform A	A0A151NCL4_ALLM	7	295
Complement C1q subcomponent subunit C	A0A151N005_ALLMI	4	290
Uncharacterized protein	A0A151MFZ6_ALLM	5	271
Zinc finger and BTB domain-containing protein 4	A0A151MYL8_ALLM	I 5	265
Complement C1q subcomponent subunit A	A0A151MZN0_ALLM	1 4	245
Keratin, type I cytoskeletal 19	A0A151PC64_ALLMI		234
Haptoglobin	A0A151MVG5_ALLM	II 4	228
lg-like domain-containing protein	A0A151NG86_ALLM	I 3	206
C4b-binding protein alpha chain-like	A0A151MAQ5_ALLN	II 5	206
Serpin peptidase inhibitor, clade A (Alpha-1 antiproteinase, antitrypsin), member 4	A0A151P987_ALLMI	5	201
Ovostatin-like protein 1-like	A0A151MRY5_ALLM	I 3	198
Adiponectin	A0A151M626_ALLM		181
Ig-like domain-containing protein	A0A151M7S2_ALLM	1 2	176
Plasma protease C1 inhibitor	A0A151NVG0_ALLM	I 3	173
Uncharacterized protein	A0A151NG84_ALLM	1 3	173
Stanniocalcin-2	A0A151M6X4_ALLM	1 3	168
Pantetheinase	A0A151M3D7_ALLM	I 3	162
Uncharacterized protein	A0A151MFZ3_ALLM	3	155

(Continued) (Continued)

TABLE 1 | Continued

Protein name	Symbol	Sequences	Total score (p < 0.05) [†]
Retinoic acid receptor responder protein 2	A0A151LYA0_ALLMI	2	161
Protein AMBP	A0A151MF04 ALLMI	2	139
lg-like domain-containing	A0A151P541_ALLMI		138
protein V-set domain-containing T-cell activation inhibitor 1-like	A0A151MVY5_ALLM	I 3	137
Protein Z-dependent protease inhibitor	A0A151P8Q1_ALLMI	3	135
Fibrinogen C-terminal domain-containing protein	A0A151MF29_ALLMI	2	134
Ig-like domain-containing protein	A0A151P538_ALLMI	2	133
Vitelline membrane outer layer 1-like protein	A0A151PFR3_ALLMI	3	132
Apolipoprotein A-IV	A0A151LZQ0_ALLMI	2	131
Ig-like domain-containing protein	A0A151NR11_ALLMI	2	131
Keratin, type I cytoskeletal 14	A0A151PC58_ALLMI	3	130
Vitronectin	A0A151NVP9_ALLMI	2	130
Sushi domain-containing protein	A0A151P1M1_ALLM	2	129
Uncharacterized protein	A0A151MP64_ALLM	3	126
Disabled-like protein 1 isoform B	A0A151M4I5_ALLMI	2	121
Beta-2-glycoprotein 1	A0A151N2D1_ALLM	2	120
Ig-like domain-containing protein	A0A151M7W3_ALLN	11 1	118
Complement component C8 alpha chain	A0A151M4H1_ALLM	1 2	113
Histidine-rich glycoprotein	A0A151M7M7_ALLN	1 2	112
Chondroadherin isoform A	A0A151N2Q4_ALLM	2	109
Ig-like domain-containing protein	A0A151M7N2_ALLM	l 1	108
Complement factor H-related protein 3-like	A0A151NBK6_ALLM	3	108
Uncharacterized protein (apolipoprotein E-like)	A0A151N395_ALLMI	2	105
Ig-like domain-containing protein	A0A151P518_ALLMI	2	104
Alpha-1-antitrypsin-like	A0A151P8V8_ALLMI	2	94
Ig heavy chain V region 6.96	A0A151P441_ALLMI	2	93
Leucine-rich alpha-2-glycoprotein	A0A151MCJ2_ALLM	1 2	90
Uncharacterized protein	A0A151MAL5_ALLM	2	88
lg-like domain-containing protein	A0A151P518_ALLMI	2	86
Alpha-1-antiproteinase-like	A0A151P8W0_ALLM	1 2	82
Insulin-like growth factor-binding protein complex acid labile subunit	A0A151N6V5_ALLMI	2	78
Apolipoprotein B-100	A0A151PIT1_ALLMI	3	77
Properdin	A0A151MYJ4_ALLMI	2	77

TABLE 1 | Continued

Complement component C7 A0A151MX90_ALLM Anionic trypsin-2-like A0A151NL42_ALLM Angiogenin A0A151MM94_ALLM N-Acetylmuramoyl-I-alanine amidase Ig-like domain-containing protein GRIP and coiled-coil A0A151NXH0_ALLM domain-containing protein 2 Fibulin-1 A0A151P794_ALLM	1	75 75 73 72 72 72 69
Angiogenin A0A151MM94_ALLM N-Acetylmuramoyl-I-alanine amidase Ig-like domain-containing protein GRIP and coiled-coil A0A151NXH0_ALLM domain-containing protein 2 Fibulin-1 A0A151P794_ALLM	1	73 72 72 69
N-Acetylmuramoyl-l-alanine amidase Ig-like domain-containing protein GRIP and coiled-coil domain-containing protein 2 Fibulin-1 A0A151PH98_ALLM A0A151N4A7_ALLM A0A151NXH0_ALLM A0A151P794_ALLM	1 2 1 2 1 2 1 2 2 2	72 72 69
amidase Ig-like domain-containing protein GRIP and coiled-coil A0A151NXH0_ALLM domain-containing protein 2 Fibulin-1 A0A151P794_ALLM	2 11 2 1 2	72 69
Ig-like domain-containing protein GRIP and coiled-coil A0A151NXH0_ALLM domain-containing protein 2 Fibulin-1 A0A151P794_ALLM	1 2 2	69
domain-containing protein 2 Fibulin-1 A0A151P794_ALLM	l 2 2	
Fibulin-1 A0A151P794_ALLM	2	66
	_	
Complement C2 A0A151PIR2_ALLMI		63
Selenoprotein P A0A151MWX0_ALLN	ЛI 2	54
Ig-like domain-containing A0A151P973_ALLM protein	l 1	54
Ig-like domain-containing A0A151MRI0_ALLM protein	l 1	53
Pericentrin isoform D A0A151N9S1_ALLM	1 2	53
Uncharacterized protein A0A151NLI3_ALLMI	2	53
AT-rich interactive A0A151MAK9_ALLN domain-containing protein 3B	11 2	52
Laminin subunit beta-3 A0A151MJP2_ALLN isoform A	11 2	51
Uncharacterized protein A0A151NFR7_ALLM	II 1	51
Signal transducer and A0A151PC08_ALLM activator of transcription	1 2	51
ZZ-type zinc A0A151NJ96_ALLM finger-containing protein 3 isoform B	1 2	50
Ig-like domain-containing A0A151NR16_ALLM protein	II 1	49
WD repeat-containing protein A0A151NU67_ALLN 11 isoform C	ll 2	48
Avidin-like A0A151MRC9_ALLN		47
Complement factor B A0A151PIT0_ALLMI	1	47
Uncharacterized protein A0A151MF67_ALLM		46
Complement factor H-like A0A151NLD7_ALLM		46
Uncharacterized protein A0A151MT59_ALLM		44
Uncharacterized protein A0A151NT34_ALLM Sulfhydryl oxidase A0A151MIB1_ALLM		44 42
Exostosin-like 1 isoform B A0A151MMH5_ALLM		42
Putative E3 ubiquitin-protein A0A151P8Y0_ALLM ligase UBR7		41
Sorbitol dehydrogenase A0A151MAA7_ALLN	11 1	41
Carboxypeptidase B2 A0A151MHY8_ALLN		40
T-complex protein 1 subunit A0A151MYL4_ALLN eta	11 1	40
BTB/POZ domain-containing A0A151P8X9_ALLM protein 7	l 1	39
Citron Rho-interacting kinase A0A151N4K3_ALLM isoform B	ll 1	39
Uncharacterized protein A0A151ND16_ALLN		39
Prickle-like protein 1 A0A151PEZ2_ALLM isoform A		39
Ras-related protein Rab-17 A0A151N9P9_ALLM isoform B	ll 1	38

(Continued)

(Continued)

TABLE 1 | Continued

Protein name	Symbol	Sequences	Total score $(p < 0.05)^{T}$
Uncharacterized protein	A0A151LZX4_ALLMI	1	38
T-lymphoma invasion and	A0A151ME23_ALLM	l 1	38
metastasis-inducing protein 1			
Uncharacterized protein	A0A151NRI7_ALLMI	1	38
Neuronal PAS domain-containing protein 3 isoform A	A0A151NKE6_ALLM	1 1	37
Ankyrin repeat domain-containing protein 26 isoform A	A0A151PEV8_ALLMI	1	37
Cadherin-1	A0A151P0T5_ALLMI	1	36
Ig-like domain-containing protein	A0A151NR67_ALLM	1 1	34
Uncharacterized protein	A0A151M2C1_ALLM	1 1	34
Zinc finger castor-like protein 1 isoform C	A0A151N3T3_ALLMI	1	34
Ubiquitin carboxyl-terminal hydrolase 8 isoform C	A0A151M9E3_ALLM	l 1	33
Uncharacterized protein	A0A151P059_ALLMI	1	33
Arf-GAP with coiled coil, ANK repeat, and PH domain-containing protein 1	A0A151N149_ALLMI	1	33
Membrane-bound transcription factor site-1 protease	A0A151MLJ3_ALLMI	1	33
TRAF family member-associated NF-kappa-B activator	A0A151M0A1_ALLM	l 1	32
Pyruvate carboxylase, mitochondrial	A0A151PCD5_ALLM	l 1	32
Leukocyte receptor cluster member 8	A0A151N898_ALLMI	1	32

Deiminated proteins in alligator plasma were isolated by immunoprecipitation using the pan-deimination F95 antibody. The resulting F95-enriched eluate was then analysed by LC-MS/MS and peak list files submitted to mascot. Alligator mississippiensis species-specific peptide sequence hits are listed (ALLMI), showing number of sequences for protein hits and total score. Blue highlighted rows indicate protein hits identified in whole plasma only (for full details on protein hits see **Supplementary Table 1**).

 † lons score is $-10 \times \text{Log}(P)$, where P is the probability that the observed match is a random event. Individual ions scores >32 indicated identity or extensive homology (p < 0.05). Protein scores were derived from ions scores as a non-probabilistic basis for ranking protein hits.

The resulting F95-enriched eluate was then analyzed by LC-MS/MS and peak list files submitted to mascot. *Alligator mississippiensis* species-specific peptide sequence hits are listed (ALLMI), showing the number of sequences for protein hits and total score. Blue highlighted rows indicate protein hits identified in whole plasma only (for full details on protein hits, see **Supplementary Table 1**).

Protein-Protein Interaction Network Identification of Deiminated Proteins in Plasma and EVs

For the prediction of protein-protein interaction networks of these deimination candidate proteins, the protein ID lists

TABLE 2 Deiminated proteins in plasma extracellular vesicles (EVs) of alligator (*Alligator mississippiensis*), as identified by F95 enrichment.

Protein name	Symbol	Sequences	Total score $(p < 0.05)^T$
Uncharacterized protein (complement C3)	A0A151NL74_ALLMI	62	3,704
Uncharacterized protein	A0A151NFJ9_ALLMI	43	2,719
Serum albumin	A0A151N5S7_ALLMI	32	1,711
Fibrinogen alpha chain	A0A151PBF3_ALLMI	25	1,672
Fibrinogen beta chain	A0A151PC06_ALLMI	25	1,526
Alpha-2-macroglobulin-like	A0A151NFQ0_ALLM	1 23	1,486
Uncharacterized protein (venom factor)	A0A151NM44_ALLM	I 25	1,411
Fibrinogen gamma chain	A0A151PB79_ALLMI	22	1,305
Uncharacterized protein	A0A151N583_ALLMI	22	1,262
Uncharacterized protein	A0A151MZ64_ALLM	1 20	1,221
Kininogen-1	A0A151M678_ALLM	19	1,213
Hemopexin	A0A151NGB2_ALLM	I 18	1,107
Melanotransferrin	A0A151MJZ7_ALLMI	15	906
Uncharacterized protein	A0A151MYS3_ALLM	l 13	856
Complement receptor type 1-like	A0A151MS72_ALLM	l 15	838
Uncharacterized protein	A0A151MJS8_ALLM	I 13	791
Carbonic anhydrase 6	A0A151N4K1_ALLMI	13	736
Uncharacterized protein	A0A151NDR9_ALLM	I 13	679
Uncharacterized protein	A0A151MYV2_ALLM	l 8	656
Uncharacterized protein	A0A151PB91_ALLMI	8	637
Fetuin-B isoform B	A0A151M7P5 ALLM		576
Carbonic anhydrase 6	A0A151N4K1_ALLMI	10	540
Plasma kallikrein isoform B	A0A151PAG7_ALLM		533
Uncharacterized protein	A0A151P5P7_ALLMI		475
CD5 antigen-like	A0A151PHB7_ALLM		469
Keratin, type I cytoskeletal 19	A0A151PC64_ALLMI		445
Keratin, type I cytoskeletal 20	A0A151PC95 ALLMI		425
Uncharacterized protein	A0A151MAL5_ALLM		407
IF rod domain-containing protein	A0A151LYF4_ALLMI	8	391
Ig lambda chain V-1 region	A0A151P8L7_ALLMI	4	347
Complement factor H	A0A151NM72_ALLM		336
Hemoglobin subunit beta	A0A151PG12_ALLM		326
Keratin, type I cytoskeletal 14	A0A151PC58_ALLMI		325
T-cell surface glycoprotein CD8 beta chain	A0A151P975_ALLMI		292
Fibrinogen C-terminal domain-containing protein	A0A151MF51_ALLM	4	285
Complement C5	A0A151NUM2_ALLM	11 5	281
Plasminogen	A0A151M2C0_ALLM		259
Complement C1q	A0A151MZU2 ALLM		253
subcomponent subunit B			
Complement C1q subcomponent subunit C	A0A151N005_ALLMI	3	251
Uncharacterized protein	A0A151MYZ1_ALLM	I 5	248
Uncharacterized protein	A0A151NDR1_ALLM		236
Glutathione peroxidase	A0A151MUD9_ALLM		234
•	_		

(Continued)

TABLE 2 | Continued

Protein name	Symbol	Sequences	Total score $(p < 0.05)^{\dagger}$
IF rod domain-containing protein	A0A151LYE5_ALLMI	4	223
Uncharacterized protein	A0A151MYX2_ALLM	II 3	208
Complement C1q subcomponent subunit A	A0A151MZN0_ALLM	11 3	192
Hemoglobin subunit alpha-A	A0A151P678_ALLMI	4	181
Alpha-1-inhibitor 3-like	A0A151M7F0_ALLM	I 4	180
Uncharacterized protein	A0A151NSW8_ALLN	1 I 3	154
lg-like domain-containing protein	A0A151P538_ALLMI	3	145
Histone H4	A0A151NSZ8_ALLM	1 3	130
TED_complement domain-containing protein	A0A151N5Z3_ALLM	1 2	126
lg-like domain-containing protein	A0A151P518_ALLMI	2	126
Uncharacterized protein	A0A151MP64_ALLM	II 2	120
Antithrombin-III	A0A151MIW1_ALLM	1 2	113
Vitronectin	A0A151NVP9_ALLM	1 2	108
HATPase_c domain-containing protein	A0A151NIG2_ALLMI	1	107
Desmin	A0A151MQA4_ALLM	11 2	104
lg-like domain-containing protein	A0A151M7S2_ALLM	11 2	103
Heterogeneous nuclear ribonucleoproteins A2/B1	A0A151MQK4_ALLN	11 2	100
Ig epsilon chain C region	A0A151MYW1_ALLN	ЛI 2	97
Alpha-1-antitrypsin	A0A151P8P3_ALLM	1 2	95
Uncharacterized protein	A0A151N405_ALLM	I 3	92
I-lactate dehydrogenase	A0A151MCB3_ALLN	11 1	87
Uncharacterized protein	A0A151NG84_ALLM	1 2	87
Ovostatin-like protein 1-like	A0A151MRY5_ALLM	11 2	83
Histone H2A	A0A151LYY4_ALLMI	2	82
Heterogeneous nuclear ribonucleoprotein U	A0A151MHH8_ALLN	/I 1	80
Tubulin beta chain	A0A151MZH9_ALLM	11 2	78
Heparin cofactor 2 isoform B	A0A151MLS1_ALLM	11 2	77
Olfactory receptor	A0A151M3L3_ALLM	l 1	73
Anionic trypsin-2-like	A0A151NL42_ALLM	l 1	72
Glyceraldehyde-3-phosphate dehydrogenase	A0A151M7G4_ALLN	11 2	67
Ovoinhibitor	A0A151MEG6_ALLM	11 2	67
Glyceraldehyde-3-phosphate dehydrogenase	A0A151MCM1_ALLN	ЛI 2	66
Plasma protease C1 inhibitor	A0A151NVG0_ALLN	ll 2	63
40S ribosomal protein SA	A0A151P2K0_ALLM	l 1	61
Triosephosphate isomerase	A0A151MCS3_ALLM	11 2	60
Heat-shock protein, mitochondrial	A0A151NA12_ALLM	l 1	59
Uncharacterized protein	A0A151PC76_ALLM	1 2	59
Actin filament-associated protein 1-like 2 isoform D	A0A151NUD0_ALLM	11 2	59

TABLE 2 | Continued

Protein name	Symbol	Sequences	Total scor (p < 0.05)
Tr-type G domain-containing protein	A0A151MMV6_ALLN	ЛI 1	59
Desmoplakin	A0A151ND53_ALLM	11 2	58
Uncharacterized protein	A0A151NLW7_ALLM	11 2	57
lg-like domain-containing protein	A0A151MRI0_ALLMI	1	55
Tubulin alpha chain	A0A151N6Z6_ALLM	l 1	53
Fibrinogen C-terminal domain-containing protein	A0A151MF29_ALLM	1	53
Serpin peptidase inhibitor, clade A (Alpha-1 antiproteinase, antitrypsin), member 4	A0A151P987_ALLM	l 1	51
Vitamin D-binding protein	A0A151N541_ALLM	1 2	50
60S ribosomal protein L23a	A0A151MUP1_ALLN	1 1	47
Tropomyosin alpha-1 chain isoform	A0A151MA07_ALLM	11 1	46
Kinesin motor domain-containing protein	A0A151M9A9_ALLM	11 2	46
Selenoprotein P	A0A151MWX0_ALLN	ЛI 1	45
Golgin subfamily A member 3 isoform A	A0A151NRP7_ALLN	11 2	43
Serine incorporator 4	A0A151M668_ALLM	ll 1	42
Cleavage and polyadenylation specificity factor subunit 6 isoform B	A0A151PFC7_ALLM	l 1	42
Protein AHNAK2	A0A151MYU6_ALLN	1 1	41
Uncharacterized protein	A0A151M202_ALLM	ll 1	40
BTB/POZ domain-containing protein 7	A0A151P8X9_ALLM	l 1	40
IgGFc-binding protein-like	A0A151MJC3_ALLM	11 1	40
60S ribosomal protein L11 isoform A	A0A151MML3_ALLN	/II 1	40
Steroid 17-alpha-hydroxylase/17,20 lyase	A0A151NV24_ALLM	1 2	39
Small G protein signaling modulator 1 isoform B	A0A151NSF2_ALLM	l 1	39
lg-like domain-containing protein	A0A151N4A7_ALLM	l 1	39
TRAF family member-associated NF-kappa-B activator	A0A151M0A1_ALLM	11 1	38
40S ribosomal protein S26	A0A151NSA5_ALLN	ll 1	38
Coagulation factor XII	A0A151NM16_ALLN	11 1	38
Sushi domain-containing protein	A0A151NM16_ALLM	11 1	37
Complement factor H-related protein 3-like	A0A151NBK6_ALLN	11 1	36
Cadherin-1	A0A151P0T5_ALLM	l 1	36
Histidine-rich glycoprotein TED_complement	A0A151M7M7_ALLN A0A151M7E8_ALLN		34 34

(Continued)

(Continued)

TABLE 2 | Continued

Protein name	Symbol	Sequences	Total score (p < 0.05) [†]
Zinc finger castor-like protein 1 isoform C	A0A151N3T3_ALLM	ll 1	34
V-set domain-containing T-cell activation inhibitor 1-like	A0A151MVY5_ALLN	/II 1	34
C4b-binding protein alpha chain-like	A0A151MAQ5_ALLN	ЛI 1	33
Neuronal PAS domain-containing protein 3 isoform A	A0A151NKE6_ALLM	11 1	33
Arf-GAP with coiled-coil, ANK repeat and PH domain-containing protein 1	A0A151N149_ALLM	ll 1	33
Tubulin alpha-2 chain	A0A151LY82_ALLM	1 1	32

Deiminated proteins from EVs were isolated by immunoprecipitation using the pandeimination F95 antibody. The resulting F95-enriched eluate was then analyzed by LC-MS/MS and peak list files submitted to mascot. Alligator mississippiensis species-specific peptide sequence hits are listed (ALLMI), showing the number of sequences for protein hits and total score. Rows highlighted in pink indicate protein hits identified in plasma EVs only (for full details on protein hits, see **Supplementary Table 2**).

[†]Ions score is $-10 \times \text{Log}(P)$, where P is the probability that the observed match is a random event. Individual ions scores >32 indicated identity or extensive homology (p < 0.05). Protein scores were derived from ions scores as a non-probabilistic basis for ranking protein hits.

for plasma and plasma EVs, respectively, were submitted to STRING analysis (https://string-db.org/) (Figures 4–7). Protein interaction networks were based on known and predicted interactions and represent all deiminated proteins identified in plasma (Figure 4), all deiminated proteins identified in EVs (Figure 5), as well as deiminated proteins identified in plasma only (Figure 6) or in EVs only (Figure 7). The proteinprotein interaction (PPI) enrichment p-value for all deiminated proteins identified in alligator plasma (based on protein identifier sequences) was found to be $p < 1.0 \times 10^{-16}$, and for all deiminated proteins identified in the plasma-derived EVs, the PPI enrichment p-value was also found to be p < 1.0 \times 10⁻¹⁶ (**Figures 4**, **5**). For deiminated proteins identified in plasma only (but not EVs), the PPI enrichment p-value was also $p < 1.0 \times 10^{-16}$ (Figure 6), while for deiminated proteins identified specifically in EVs, the PPI enrichment pvalue was $p = 4.83 \times 10^{-8}$ (Figure 7). This indicates that, in all cases, the identified protein networks have significantly more interactions than expected for a random set of proteins of similar size, drawn from the genome. The Kyoto Encyclopedia of Genes and Genomes (KEGG) pathways related to deiminated proteins identified as deiminated in whole plasma only, related to the adipocytokine signaling pathway (Figure 6E), based on STRING analysis for A. mississippiensis, while deiminated proteins identified as deiminated in EVs only belonged to KEGG pathways for ribosome, biosynthesis of amino acids, and glycolysis/gluconeogenesis (**Figure 7E**). Protein families (PFAM) protein domains differed for deamination-specific proteins in plasma compared to in EVs (Figures 6B, 7B), as did Simple

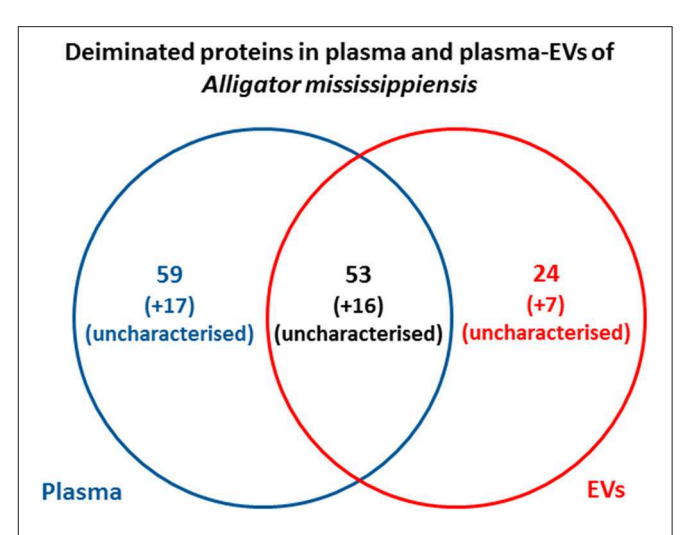


FIGURE 3 | Deiminated proteins identified in alligator plasma and plasma extracellular vesicles (EVs). Species-specific hits identified for deiminated proteins in American alligator plasma and EVs showed overall 145 proteins identified in plasma and 100 in EVs. Of these, 69 protein hits were overlapping, while 76 proteins were specific for whole plasma and 31 for plasma EVs only, respectively.

Modular Architecture Research Tool (SMART) protein domains, which for plasma showed serpin, trypsin, and complement-related domains [von Willebrand factor (vWF) and membrane attack complex (MAC)/perforin domains], while EVs showed also core histone domains (**Figures 6C**, **7C**). STRING analysis for UniProt keywords, INTERPRO [http://www.ebi.ac.uk/interpro/; (92)] protein domains and features are furthermore highlighted for plasma and plasma EVs (**Figures 4–7**).

Phylogeny Tree for American Alligator PADs Compared to Human PADs

A phylogeny tree for American alligator reported and predicted PAD sequences (PAD1, 2, and 3) compared to human PADs 1, 2, 3, 4, and 6, using Clustal Omega, revealed the closest relationship between alligator PAD2 with human PAD2 (**Figure 8**). This correlates with the strongest cross-reaction detected with the antihuman PAD2 antibody in both alligator plasma and plasma EVs (**Figure 2**).

DISCUSSION

The current study is the first to profile deiminated proteins in plasma and EVs of American alligator (*A. mississippiensis*), and the first such study of a non-avian diapsid (extant reptiles). F95 enrichment revealed a range of immunological, metabolic, and gene regulatory proteins as candidates for this posttranslational modification, therefore indicating hitherto underrecognized modes for protein moonlighting of these proteins in alligator physiology and immunity. PAD proteins were identified in alligator plasma via cross-reaction to antibodies raised against human PAD isozymes (PAD2, 3, and 4), which were previously shown to cross-react with PADs with diverse taxa, and such

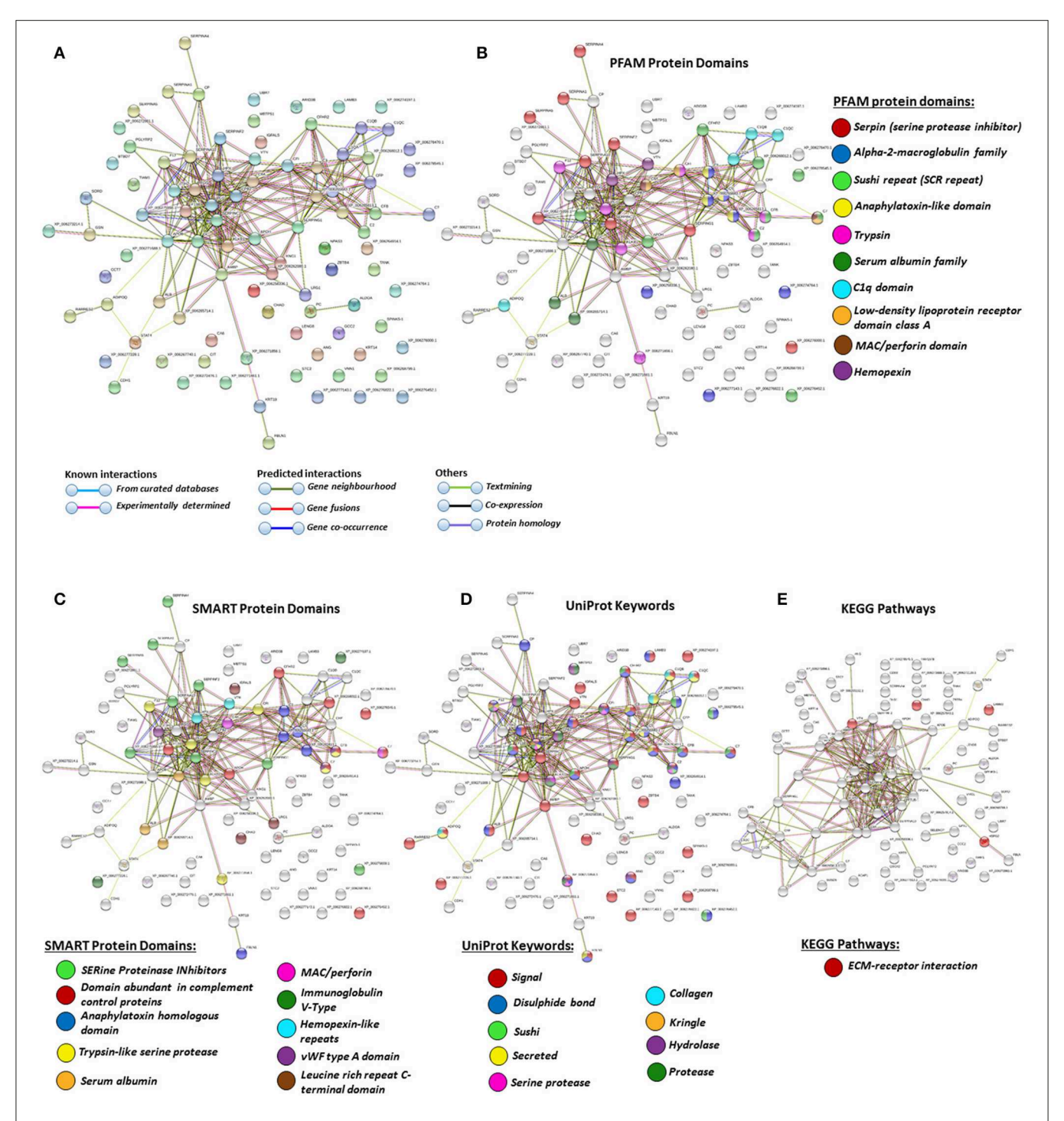


FIGURE 4 | Protein-protein interaction networks of all deiminated proteins identified in alligator plasma. Reconstruction of protein-protein interactions based on known and predicted interactions in Alligator mississippiensis, using Search Tool for the Retrieval of Interacting Genes/Proteins (STRING) analysis. (A) Colored nodes represent query proteins and first shell of interactors. (B) Protein families (PFAM) protein domains relating to the identified proteins and reported in STRING are highlighted for: serpin, alpha-2-macroglobulin family, sushi repeat, anaphylatoxin-like domain, trypsin, serum albumin family, C1q domain, low-density lipoprotein (LDL)-receptor domain class A, membrane attack complex (MAC)/perforin domain, and hemopexin (see color code included in the figure). (C) Simple Modular Architecture Research Tool (SMART) protein domains relating to the identified proteins and reported in STRING are highlighted for serine proteinase inhibitors, domain abundant in complement control proteins, anaphylatoxin homologous domain, trypsin-like serine protease, serum albumin, MAC/perforin, Ig V-type, hemopexin-like repeats, von Willebrand factor (WF) type A domain, and leucine-rich repeat C-terminal domain (see color code included in the figure). (D) UniProt keywords relating to the identified proteins and reported in STRING are highlighted for: signal, disulfide bond, sushi, secreted, serine protease, collagen, kringle, hydrolase, and protease (see color code included in the figure). (E) KEGG pathways relating to the identified proteins and reported in STRING are highlighted as follows: red = ECM-receptor interactions (corrated databases, experimentally determined), predicted interactions (gene neighborhood, gene fusion, gene co-occurrence), or via text mining, coexpression, or protein homology (see the color key for connective lines included in the figure).

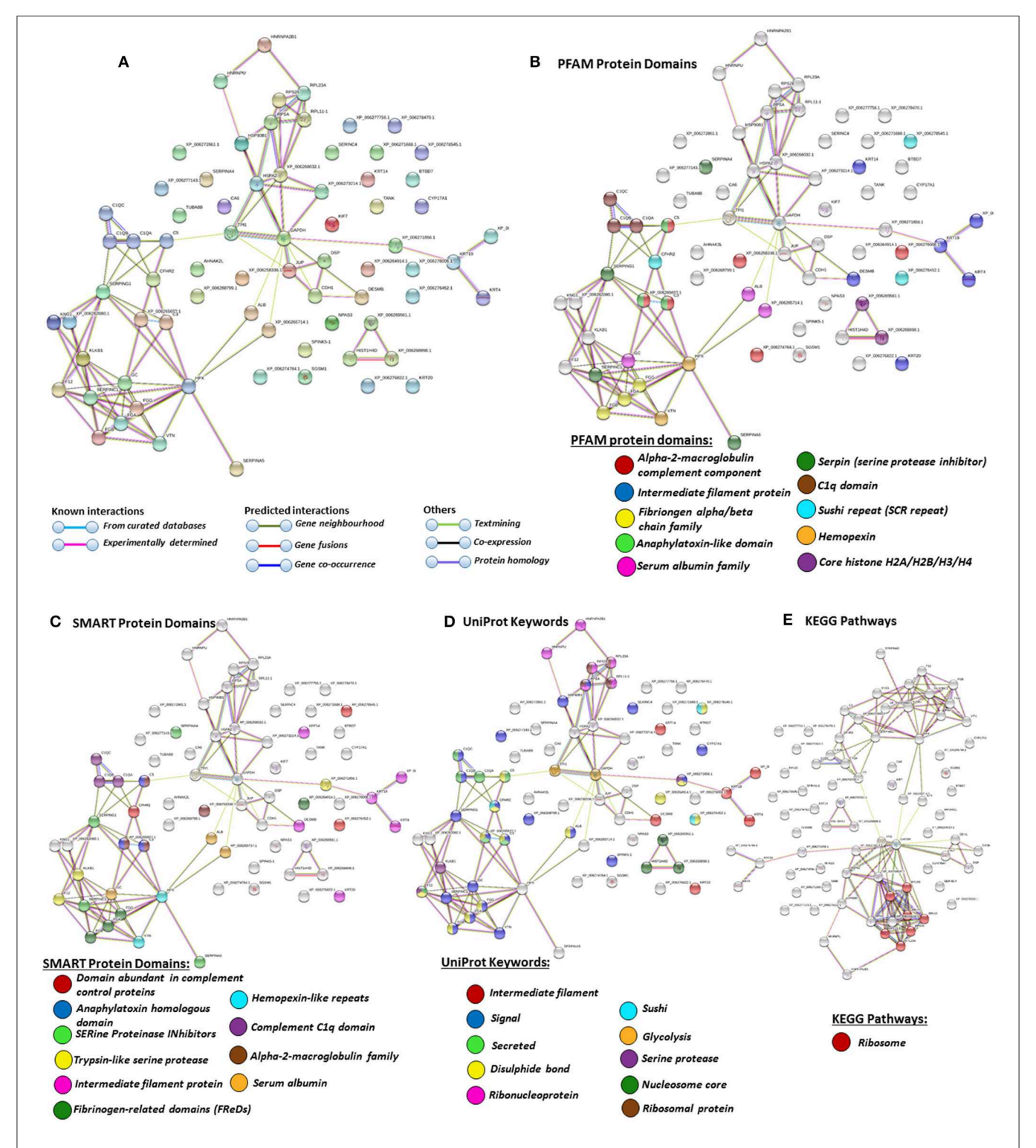


FIGURE 5 | Protein-protein interaction networks of all deiminated proteins identified in plasma extracellular vesicles (EVs) of Alligator mississippiensis. Reconstruction of protein-protein interactions based on known and predicted interactions using the Search Tool for the Retrieval of Interacting Genes/Proteins (STRING) analysis.

(A) Colored nodes represent query proteins and first shell of interactors. (B) Protein families (PFAM) protein domains relating to the identified proteins and reported in STRING are highlighted as follows: alpha-2-macroglobulin family, intermediate filament protein, fibrinogen chain family, anaphylatoxin-like domain, serum albumin family, serpin, C1q domain, sushi repeat, hemopexin, and core histones (see color code included in the figure). (C) SMART protein domains relating to the identified proteins and reported in STRING are highlighted as follows: domain abundant in complement control proteins, anaphylatoxin homologous domain, serine proteinase (Continued)

FIGURE 5 | inhibitors, trypsin-like serine protease, intermediate filament protein, fibrinogen-related domains, hemopexin-like repeats, C1q domain, alpha-2-macroblobulin family, and serum albumin (see color code included in the figure). **(D)** UniProt keywords relating to the identified proteins and reported in STRING are highlighted as follows: intermediate filament, signal, secreted, disulfide bond, ribonucleoprotein, sushi, glycolysis, serine protease, nucleosome core, ribosomal protein (see color code included in the figure). **(E)** Kyoto Encyclopedia of Genes and Genomes (KEGG) pathways relating to the identified proteins and reported in STRING are highlighted as follows: red = ribosome. Colored lines indicate whether protein interactions are identified via known interactions (curated databases, experimentally determined), predicted interactions (gene neighborhood, gene fusion, gene co-occurrence), or via text mining, coexpression, or protein homology (see the color key for connective lines included in the figure).

detection is in accordance with that PADs have previously reported in the alligator genome (PADI1, Gene ID: 102574884; PADI2, Gene ID: 102575591; PADI3, Gene ID: 102574651). The antihuman PAD2 antibody showed strongest cross-reaction with alligator plasma proteins at a predicted size of 70–75 kDa for PAD proteins, also in the plasma EVs, and this is in accordance with previous findings reporting PAD2 to be the most phylogenetically conserved isozyme (14, 56, 58, 76, 77, 79), as also confirmed by the cladogram constructed based on sequence alignment of predicted and reported protein sequences for alligator and human PAD isozymes (Figures 8A,B). Furthermore, the difference detected in cross-reaction with antihuman PAD2, PAD3, and PAD4 antibodies (note that neither antihuman PAD1 nor PAD6 antibodies were assessed here) in whole plasma compared with plasma EVs, as PAD4 did not show positive in the EVs, may be associated with the differences observed in deiminated protein targets in plasma vs. plasma EVs. Preferences for the different PAD isozymes against cellular substrates is indeed known (93). The presence of deiminated histone H3 (citH3), which sometimes is used as a marker of NETosis was also identified here by Western blotting in alligator plasma, providing the first evidence of PAD-mediated NETosis mechanisms in reptiles, although other circulating histones have previously been identified in crocodilian blood (94). While NETosis has been shown to be a phylogenetically conserved mechanism from fish to mammals (95), the only other studies on NETosis related to reptiles have been investigations on snake venom, showing that Indian saw-scaled viper (Echis carinatus) venom induces neutrophil extracellular trap (NET) formation in host tissue, through which it contributes to tissue destruction of the affected area (96, 97). It has to be noted though that further evaluation of NETosis in alligator plasma will need to be performed, as the direct link between histone citrullination/deimination and NETosis has been challenged (98).

A number of alligator species-specific deiminated protein candidates were identified in both plasma and plasma-derived EVs, using F95 enrichment in tandem with LC-MS/MS analysis. This analysis revealed some key metabolic and immune-related proteins, with 53 characterized common deiminated proteins in plasma and EVs, while 59 characterized deiminated protein hits were specific for plasma and 24 characterized deiminated protein hits were specific for EVs. Upon assessment of protein-protein interaction networks using STRING analysis, the PPI enrichment *p*-value for all deiminated proteins identified in alligator plasma and in plasma EVs, as well as for deiminated proteins identified either in plasma or EVs only, indicated that the identified protein networks have significantly more interactions than expected for a random set of proteins of similar size, drawn from the genome,

and that the proteins are at least partially biologically connected, as a group (**Figures 4**–7).

In plasma, deiminated protein targets identified belonged to KEGG pathways for extracellular matrix (ECM)receptor interaction and adipocytokine signaling pathway (Figures 4E, 6E). ECM-receptor interactions control both directly and indirectly a range of cellular activities including migration, adhesion, differentiation, apoptosis, and proliferation and have been studied in cancer, also at the transcriptome level (99). KEGG pathways for ECM-receptor interaction have, for example, been previously identified to be enriched in EVs of mesenchymal stem cells (100), but regulation via posttranslational deimination has not been investigated. A recent study identified enrichment of deiminated proteins in KEGG pathways for ECM-receptor interactions in the fin whale, also long-lived cancer-resistant animal (75). Interestingly, deimination of KEGG pathways of ECM-receptor interactions has also been identified by our group in the wandering albatross (Diomedea exulans) (80), which emphasizes the phylogenetic relationship between reptiles and birds, while exact phylogenetic reconstructions can though vary according to genomic or protein parameters used, partly also due to convergent evolution (101).

The adipocytokine signaling pathway plays important roles in metabolic regulation and is involved in a range of pathologies including insulin resistance and type II diabetes (102, 103). Adiponectin is one of the cytokines secreted by adipocytes and was here identified in alligator whole plasma only. Adiponectin has key functions in regulating glucose (104–106) and is also linked to regenerative functions (107), longevity (108), cancer (109), and myopathies (110). It has recently been identified as a deimination candidate in several taxa with unusual metabolism including the llama (*Lama glama*), the naked mole rat (*Heterocephelus glaber*), and orca (*Orcinus orca*) (75, 76, 79).

In alligator plasma EVs, F95 target proteins identified as deiminated proteins belonged to ribosomal, biosynthesis of amino acids, and glycolysis/glyconeogenesis KEGG pathways (Figures 5E, 7E). Furthermore, STRING analysis was carried out on deiminated protein hits found specifically in EVs only as well as for those only found in plasma, excluding overlapping protein hits (Figures 6, 7). This revealed enrichment of deiminated proteins in plasma linked to KEGG pathways of adipocytokine signaling (Figure 6), while in EVs, pathways related to ribosomal, biosynthesis of amino acids, and glycolysis/gluconeogenesis were enriched in deiminated proteins (Figure 7). In EVs, histone pathways were also enriched, alongside vWF and intermediate filament protein domains,

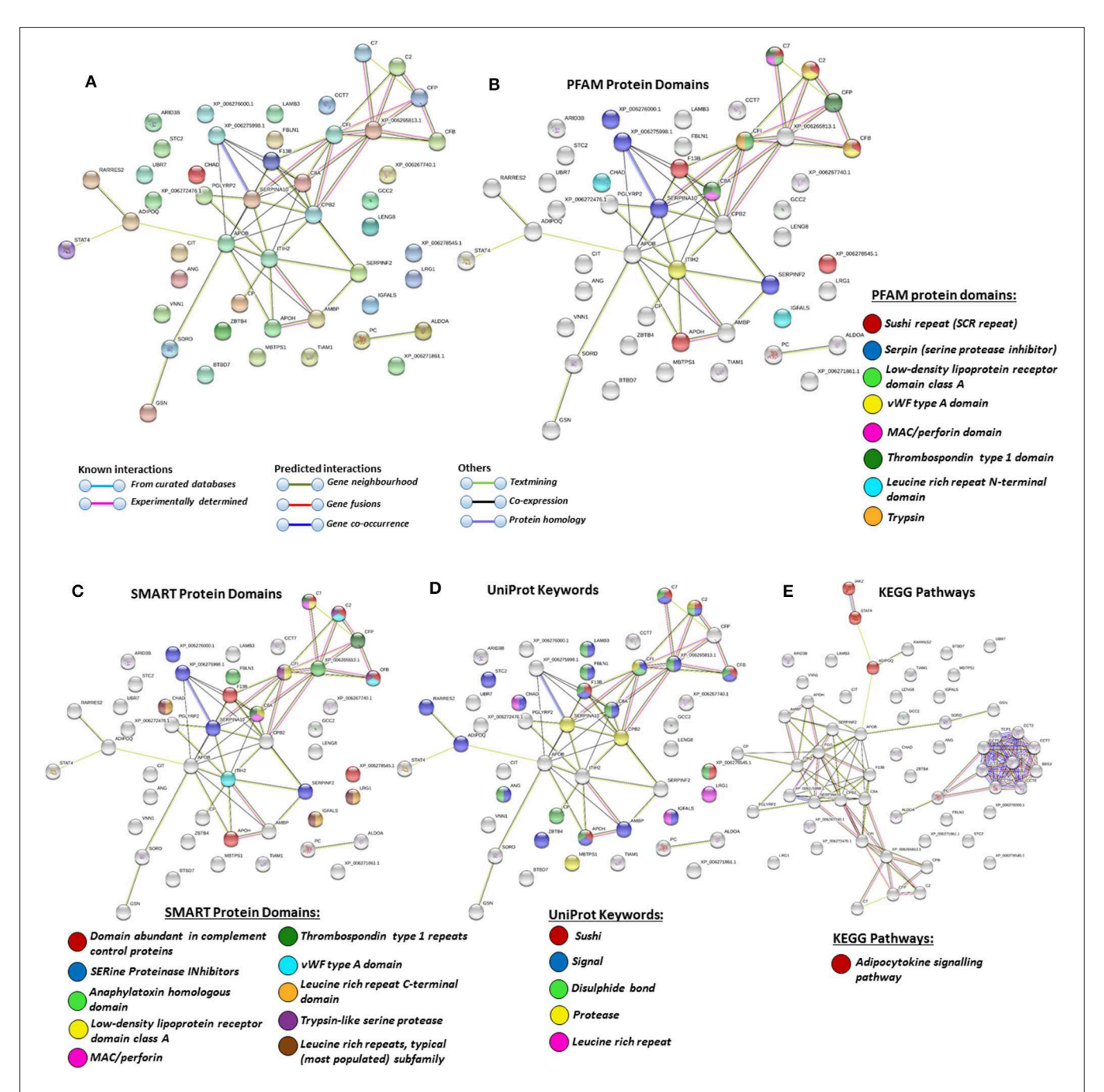


FIGURE 6 | Protein-protein interaction networks of deiminated protein candidates identified in alligator plasma only (not identified in extracellular vesicles (EVs). Reconstruction of protein-protein interactions based on known and predicted interactions using the Search Tool for the Retrieval of Interacting Genes/Proteins (STRING) analysis. (A) Colored nodes represent query proteins and first shell of interactors. (B) Protein families (PFAM) protein domains relating to the identified proteins and reported in STRING are highlighted as follows: sushi repeat, serpin, low-density lipoprotein (LDL)-receptor domain class A, von Willebrand factor (WF) type A domain, membrane attack complex (MAC)/perforin domain, thrombospondin type 1 domain, leucine-rich repeat N-terminal domain, and trypsin (see color code included in the figure). (C) Simple Modular Architecture Research Tool (SMART) protein domains relating to the identified proteins and reported in STRING are highlighted as follows: domain abundant in complement control proteins, serine proteinase inhibitors, anaphylatoxin homologous domain, LDL-receptor domain class A, MAC/perforin, thrombospondin type 1 repeats, WF type A domain, leucine-rich repeat C-terminal domain, trypsin-like serine protease, leucine-rich repeats (see color code included in the figure). (D) UniProt keywords relating to the identified proteins and reported in STRING are highlighted as follows: sushi, signal, disulfide bond, protease, leucine-rich repeat (see color code included in the figure). (E) Kyoto Encyclopedia of Genes and Genomes (KEGG) pathways relating to the identified proteins and reported in STRING are highlighted as follows: sushi, signal, disulfide proteins and reported in STRING are highlighted as follows: red = adipocytokine signaling pathways.

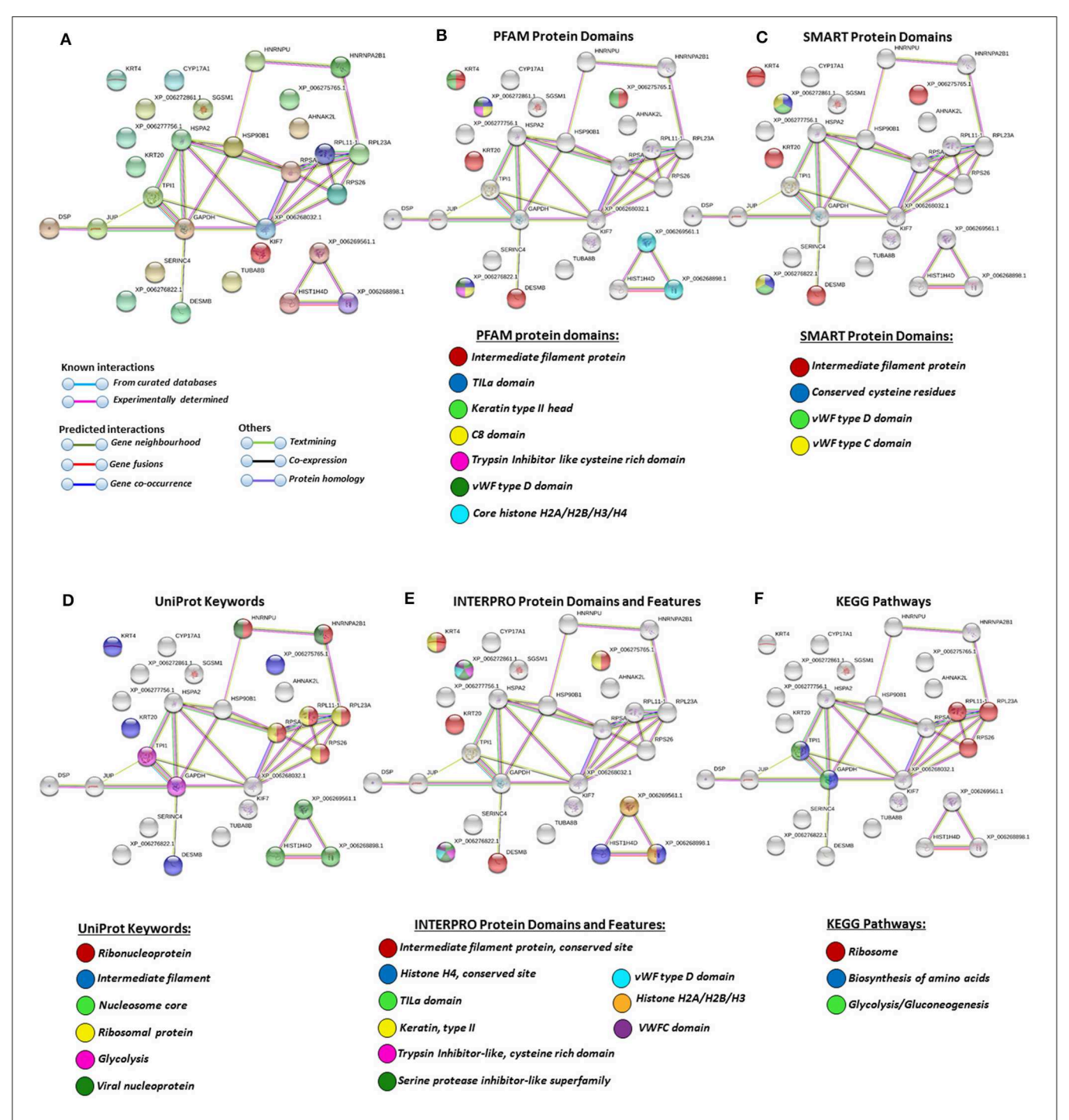


FIGURE 7 | Protein—protein interaction networks of deiminated protein candidates identified in alligator extracellular vesicles (EVs) only (not identified in total plasma). Reconstruction of protein—protein interactions based on known and predicted interactions using the Search Tool for the Retrieval of Interacting Genes/Proteins (STRING) analysis. (A) Colored nodes represent query proteins and first shell of interactors. (B) Protein families (PFAM) protein domains relating to the identified proteins and reported in STRING are highlighted as follows: intermediate filament protein, TILa domain, keratin type II head, C8 domain, trypsin inhibitor-like cysteine-rich domain, von Willebrand factor (VWF) type D domain, core histones H2A/H2B/H3/H4 (see color code included in the figure). (C) Simple Modular Architecture Research Tool (SMART) protein domains relating to the identified proteins and reported in STRING are highlighted as follows: intermediate filament protein, conserved cysteine residues, WF type D domain, and vWF type C domain (see color code included in the figure). (D) UniProt keywords relating to the identified proteins and reported in STRING are highlighted as follows: ribonucleoprotein, intermediate filament, nucleosome core, ribosomal protein, glycolysis, and viral nucleoprotein (see color code in legend). (E) INTERPRO protein domains and features: intermediate filament protein conserved site, histone H4, TILa domain, keratin type II, trypsin inhibitor-like cysteine-rich domain, serine protease inhibitor-like superfamily, vWF type D domain, histone H2A/H2B/H3, von Willebrand factor type C (WWFC) domain (see color code included in the figure). (F) Kyoto Encyclopedia of Genes and Genomes (KEGG) pathways relating to the identified deiminated proteins and reported in STRING are highlighted as follows: ribosome, biosynthesis of amino acids, and glycolysis/gluconeogenesis.

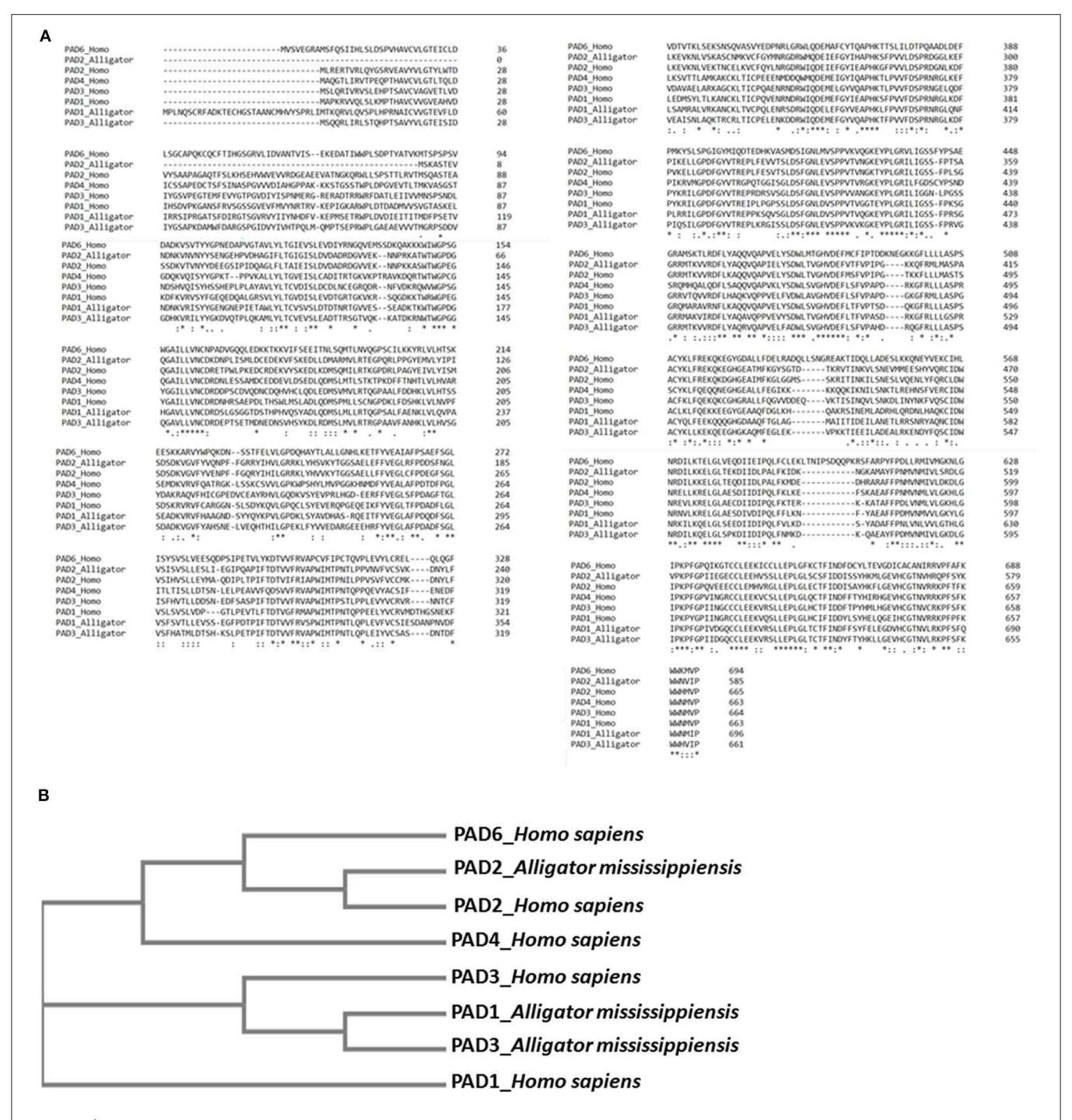


FIGURE 8 | Sequence alignment and phylogeny tree for alligator peptidylarginine deiminases (PADs) compared with human PADs. (A) Multiple sequence alignment of reported (predicted) alligator PAD sequences PAD1 (XP_006259278.3), PAD2 (XP_019355592.1), and PAD3 (XP_014457295.1) isozymes, compared with human PAD isozyme protein sequences PAD1 (NP_037490.2), PAD2 (NP_031391.2), PAD3 (NP_057317.2), PAD4 (NP_036519.2), and PAD6 (NP_997304.3), using Clustal Omega. (B) A neighbor joining tree is shown for phylogenetic clustering of the reported (predicted) alligator PAD1 (XP_006259278.3), PAD2 (XP_019355592.1), and PAD3 (XP_014457295.1) isozymes, compared with human PAD isozyme protein sequences PAD1 (NP_037490.2), PAD2 (NP_031391.2), PAD3 (NP_057317.2), PAD4 (NP_036519.2), and PAD6 (NP_997304.3), using Clustal Omega.

and PFAM domains relating to the complement pathway, fibrinogen, serpins, anaphylatoxins, hemopexin, and serum albumin (Figures 5B-E, 7B-E).

KEGG ribosomal pathways are linked to cancer-associated processes (111), and putative regulation of these networks via deimination may therefore be of importance. Furthermore, in

relation to KEGG pathways for biosynthesis of amino acids, deimination-mediated changes may be of considerable interest for comparative metabolic studies, particularly as amino acid assessment for mammalian metabolism and for research into aging and disease has received some attention (112). Glycolysis is of high relevance in metabolism and cancer, and pathways for glycolysis/gluconeogenesis, identified here in alligator plasma EVs, have previously been identified in cancer cells (27) and in several species of whale (75), which are long lived and cancerresistant sea mammals. Interestingly, in the naked mole rat, also an animal with low metabolic rate, cancer resistance, and unusual longevity, deiminated proteins relevant to glycolysis were also found to be enriched in plasma EVs specifically (79). Whether deimination in these pathways identified here in alligator is of some relevance for the low metabolic rate and cancer resistance found in alligator (10) will remain to be further investigated.

Deiminated protein candidates involved in immune pathways for antipathogenic defenses, including complement related proteins, were found both in whole plasma and enriched in the plasma EVs, indicative of EV-mediated transport of deiminated protein components. This coincides with previous findings of unusual antimicrobial defenses of alligator, much higher than in human sera and likely to be complement dependent (113). Furthermore, alligator sera has also been found active against multidrug resistant bacteria such as *Acinetobacter baumanii* and *Klebsiella pneumoniae* (8), as well as amoeba (114).

A range of proteins from the complement cascade was indeed identified here as deiminated in alligator, and this has also recently been found in other species by our group (58, 73-79), including in avian species (80). The complement system bridges innate and adaptive immunity, participates in the clearance of necrotic and apoptotic cells, and forms part of the first lines of immune defenses against invading pathogens (115-119). Interestingly, properdin was here identified as deiminated in alligator plasma for the first time in any species, as this has not been shown to be a deimination candidate in other taxa studied so far. Properdin is a positive regulator of the alternative complement pathway (AP) and linked to multifaceted roles in inflammation and disease (120, 121). It is a plasma glycoprotein that stabilizes C3 and C5 convertases and initiates and positively regulates AP activity (120, 122, 123). Properdin-mediated complement activity contributes to innate and adaptive immune responses and tissue damage, and properdin has therefore also been a target for modulation in disease pathologies (120, 124). While properdin is a known glycoprotein, deimination of properdin is here described for the first time in any species and may shed a novel light on how properdin can take on its multifaceted roles, possibly also via such posttranslational changes.

The properdin target C3 was the most identified deiminated protein in the alligator plasma and EVs. C3 has recently been identified to be deiminated in our studies in a range of taxa (76, 77, 80). Furthermore, an abundance of deiminated complement components identified to be deiminated both in plasma and plasma EVs included, besides C3, complement receptor type-1, complement factor H, complement factor I, complement C1q subcomponent subunits A and C, C4b-binding protein-like,

while C2, C7, factor B, and properdin were deiminated in whole plasma only. Deimination of the various complement components, except properdin, has recently been identified by our group in teleost and cartilaginous fish (58, 76, 78), camelids (77), cetaceans (75), and birds (80). These findings indicate hitherto understudied roles for posttranslational deimination in the known diversity of complement function throughout phylogeny (125-129). Indeed, as some of the antibacterial effects of crocodile serum have been linked to the complement system (5, 113), our findings suggest that protein deimination may play hitherto unidentified roles in the known unusual antimicrobial and anti-inflammatory function of alligator (5, 130, 131), including via EV transport in cellular communication, also playing roles in complement function in homeostatic processes. Ficolin-3 was furthermore identified to be deiminated in whole alligator plasma only and is a sugar pattern recognition molecule, which forms part of mammalian immune systems (132). Ficolin-3 can activate the complement system via the lectin pathway (133), plays roles in bacterial defenses (134, 135) and autoimmunity (136, 137) and is modulated in viral infections including HIV (138). Ficolin-3 has been associated with metabolic diseases including gestational, prediabetes, and type 2 diabetes (139, 140), and identified as biomarkers in axial spondyloarthritis (141) and as a prognostic biomarker for esophageal cancer (142). Studies on ficolins in reptiles are limited, besides putative roles for veficolins in reptile venom systems (143, 144) and for ficolin superfamily proteins as snake venom metalloproteinase inhibitors (145). Deimination of ficolin-3 has been previously identified only in the naked mole rat (79), a cancer- and hypoxia-resistant animal with unusual immunity and longevity. The roles of posttranslational deimination in regulation of ficolin-mediated mechanisms may therefore be of considerable interest, including in relation to inflammatory and oncogenic pathways.

Alpha-2-macroglobulin (alpha-2-M) was found to be deiminated in alligator plasma and plasma EVs and was identified as a PFAM protein domain in both. It clears active proteases from tissue fluids and forms part of innate immunity (146). A range of protease inhibitors and proteases were furthermore identified in both plasma and plasma EVs including plasma protease C1 inhibitor (in plasma and plasma EVs) and protein Z-dependent protease inhibitor (in plasma) and membrane-bound transcription factor site-1 protease (in plasma). Alpha-2-M is conserved throughout phylogeny from arthropods to mammals and closely related complement proteins C3, C4, and C5, which are also thioester-containing proteins (115, 147, 148). Crocodilian alpha-2-M is homologous to human alpha 2-M or chicken ovomacroglobulin and has been assessed in Cuban crocodile (Crocodylus rhombifer) (149), while its structure has furthermore been assessed by electron microscopy in Crocodylus siamensis (150). While structural changes of alpha-2- and ovomacroglobulin have been assessed to some extent (151), including the identification of three intramolecular thiol ester bonds in crocodilian ovomacroglobulin, which display differential stability against external perturbations (152), structural or functional changes mediated via posttranslational deimination have not been assessed. The deimination of

alpha-2-M has recently been identified by our group in camelid and birds (77, 80).

Serpin (serine proteinase inhibitor) PFAM and SMART domains were identified as deiminated both in alligator plasma and EVs, with specific targets identified being serpin peptidase inhibitor. Such deimination may provide a novel insight into utilizing serpin-based peptides as antimicrobials against multidrug resistant pathogens (6, 7). Deimination of serpin may also be important in the human rheumatoid arthritis citrullinome, where deimination has previously been shown to modulate protease activity, resulting in downstream effects on serpin-regulated pathways (29). Furthermore, a range of apolipoproteins was identified to be deiminated in alligator whole plasma. Apolipoproteins have antimicrobial activity against a range of pathogenic bacteria (153-156), including in alligator, and have been tested for use against several multidrug-resistant bacteria (6, 7). Various apolipoproteins have recently been identified as deimination protein candidates by our group in a range of taxa (56, 58, 77), including in pelagic seabirds (80).

Hemoglobin, which was identified here as being deiminated in alligator plasma, has, alongside crude leukocyte extract and plasma, been found to have antioxidant and anti-inflammatory activities in Chinese crocodile (Crocodylus siamensis) (131). Furthermore, viral nucleoprotein was identified as a UniProt keyword connected to deiminated proteins specific to EVs only, which may be of relevance in the light of antiviral activity of alligator serum against enveloped viruses, including human immunodeficiency virus type 1 (HIV), West Nile virus (WNV), and herpes simplex virus type 1 (HSV-1) (9). Interestingly, serine incorporator 4 was identified as deiminated in alligator plasma EVs only, and serine incorporator proteins have recently been identified as novel host restriction factors implicated in HIV-1 replication (157). This highlights a hitherto unrecognized posttranslational control mechanism of various proteins involved in antiviral responses.

The presence of deiminated histone H2A and H4 was identified in alligator EVs only. This may be of some interest, as extracellular histones H2A and H4 in crocodile blood have indeed been identified to act as inhibitors of viral (HIV) infection in vitro (94). While some studies in reptiles have assessed histone deacetylation, methylation, and histone variants (158-160), as well as linking histone methylation to anoxia survival in turtles (161), studies on posttranslational deimination of histones is lacking in non-avian reptiles. Histone H3 deimination has been previously identified inked to inflammatory responses during CNS regeneration in the chicken (Gallus gallus) (40) and in hypoxic responses during CNS repair (41). Histone deimination is also known to be involved in epigenetic regulation involved in cancer (17, 20). Interestingly, a similar EV export of deiminated histones as observed in alligator plasma here was recently identified in the naked mole rat, also an unusually long-lived and cancer-resistant animal (79). Indeed, the use of non-mammalian model organisms in epigenetic research has been highlighted, including in reptiles (162), and roles for histone modifications, including deimination identified here, may be of interest, as crocodilians are also long lived, cancer and hypoxia resistant, and furthermore show unusually resistant antipathogenic responses (4, 163).

AHNAK2 is a nucleoprotein and was identified to be deiminated in alligator plasma EVs only. AHNAK is a multifaceted proteins with roles in cell architecture and migration, blood-brain barrier formation, regulation of cardiac calcium channels, and repair of muscle membranes (164). Furthermore, roles in cancer are implicated, and AHNAK has been shown to facilitate EV release in mammary carcinoma cells (165), therefore playing critical roles in EV communication in the tumor environment. AHNAK has been identified as a biomarker in several, including metastatic, cancers (166-169) and linked to drug resistance in cancer in association with viral infection (170). AHNAK has been is also related to stress-induced secretion of FGF1—a growth factor regulating carcinogenesis, angiogenesis, and inflammation (171) and to inherited peripheral neuropathy (172). AHNAK was previously identified to be deiminated in aggressive glioblastoma cells by our group (27, 61). The deimination of AHNAK identified here specifically in alligator plasma EVs may play some roles in antipathogenic resistance but will remain to be further investigated, also in relation to human pathologies.

Protein adrenomedullin binding protein-1 (AMBP) was identified as deiminated in whole alligator plasma only. AMBP is a plasma protein that binds adrenomedullin and acts as an important modulator in the biphasic septic response, including during the progression of polymicrobial sepsis (173, 174). Insights into posttranslational regulation of AMBP via deimination may therefore be of importance for the management of sepsis and is of great interest in the light of the unusual antimicrobial properties of alligator plasma.

Various Ig proteins and Ig superfamily members were identified here to be deiminated in alligator plasma and plasma EVs, confirming that Igs can be exported via EVs. Ig proteins identified common in whole plasma and plasma EVs were IgGFc-binding protein-like, Ig lambda light chain variable region, Ig epsilon chain constant region, and Ig-like domain-containing protein, while Ig heavy chain variable region was identified as deiminated only in whole plasma. Several studies have assessed Igs in crocodilians including IgH subclassencoding genes and IgM subclass switching (175), IgA evolution (176), and analysis of Ig light (L) chains, revealing a highly diverse IgL gene repertoire (3). Posttranslational modifications and such contribution to Ig diversity remains though to be studied. We have previously confirmed posttranslational deimination if Igs in several taxa, including shark, camelid, and birds (76, 77, 80), and furthermore reported EV-mediated transport of Igs in shark and camelid (76, 77). Igs play key roles in adaptive immunity and have been extensively studied in diverse taxa. Posttranslational deimination of Igs and downstream roles in Ig function have though received little attention, until recent studies in teleosts and cartilaginous fish (56, 58), camelids (77) and cetaceans (75). In human patients with rheumatoid arthritis (RA) and bronchiectasis, it has been reported that the IgG Fc region is posttranslationally deiminated (177). In the light of growing interest in elucidating Ig diversity throughout the phylogenetic tree (178-183), our finding of deimination of crocodilian Igs in the current study highlights a novel concept of diversification of Igs via such posttranslational deimination.

T-lymphoma invasion and metastasis-inducing protein 1 (TIAM1) was here identified as deiminated in alligator plasma. It is important in the regulation of cell membrane dynamics (184), involved in the regulation of phagocytosis (185) and bacterial cell invasion in the host (186). TIAM1 has also been shown to play roles in neuronal responses to oxygen and glucose deprivation (187) and has been linked to mitochondrial dysfunction in diabetic retinopathy (188, 189) as well as to retinoblastoma (190). TIAM1 promotes chemoresistance and tumor invasiveness (191), and its expression levels are positively correlated to with poor prognosis in solid cancers (192). It is associated with histone methyltransferases in epigenetic regulation for cancer progression (193). TIAM1-mediated networks are also implicated in neuroblastoma, and therefore, strategies to regulate TIAM1 have been highlighted (194). TIAM1-regulated pathways have furthermore been highlighted as targets in autoimmunity (195), including in islet β cells in health and diabetes (196, 197). While phosphorylation of TIAM1 has been studied in relation to neurological disease (198), the posttranslational deimination of TIAM1 identified here in alligator has not been identified in any species so far to our knowledge. Such deimination-mediated changes may indicate regulatory pathways of this protein with respect to hypoxia tolerance, cancer, and autoimmune pathologies as well as host-pathogen interactions. Furthermore, posttranslational deimination of TIAM may be of some relevance in the context of utilizing TIAM pathways for the generation of optogenetic tools (184).

Exostosin-like-1 (EXTL-1) was here deiminated in whole alligator plasma only. It belongs to a family of glycosyltransferases, involved in heparin sulfate and heparin biosynthesis as well as acting as tumor suppressors (199, 200). EXTL-1 has furthermore been found to have important functions in regulation of tau uptake in relation to neurodegeneration (201). The deimination of EXTL-1 identified here in whole alligator plasma may therefore be of some relevance regarding regulation of its function via such posttranslational change and has not been described in any species so far to our knowledge.

Selenoprotein P (Sepp1) was identified to be deiminated in whole alligator plasma only. It is a plasma glycoprotein, secreted mainly from liver, as well as other tissues, and it contains most of mammalian plasma selenium (202, 203). It has antioxidant properties (202). Sepp1 has roles in homeostasis and in the distribution of selenium (203). Sepp1 is believed to have phylogenetically appeared in early metazoan species, as terrestrial animals have fewer selenoproteins than marine animals, and this may partly be reflected in different functions (204). Selenoproteins have been studied in a range of non-mammalian vertebrates including agnathans and birds (205), but no studies in particular have been carried out in alligator. While Sepp1 is known to be glycosylated, its deimination has not been studied besides being recently identified in whales (75).

L-Lactate dehydrogenase was found deiminated in EVs only, and lactate dehydrogenase has previously been identified to be a hepatic biomarker in American alligator (206).

L-Lactate controls apoptosis and autophagy in tumor cells (207) and plays important roles in the tumor microenvironment, including under hypoxic conditions, and lactate dehydrogenase metabolism has been identified as a target to overcome resistance to immune therapy of tumors (208). L-Lactate dehydrogenase has previously been identified by our group to be deiminated in glioblastoma cells (27) and in plasma of naked mole rat (79) and in minke whale (75), both long-lived and cancerresistant animals. Whether posttranslational deimination may play roles in the regulation of lactate dehydrogenase metabolism, and therefore affect pro- or anticancerous responses, remains to be investigated.

Stanniocalcin-2 (STC2) was identified as deiminated in alligator whole plasma and has not been identified as a deimination candidate in other taxa studied so far. Stanniocalcin is a secreted glycoprotein, originally studied in fish as hormone regulator of serum calcium levels (209). It is expressed in a wide range of tissues and regulates various biological processes including lipid and glucose metabolism (210, 211), the growth hormone-insulin-like growth factor axis (212), as well as cellular calcium and phosphate homeostasis (213, 214). STC2 is related to growth restriction (209) and organomegaly when overexpressed at the genetic level (215). It is upregulated in response to metabolic stresses, including hypoxia conditions (216), and forms part of the unfolded protein response (217). STC2 is also a tumor marker for several cancers as well as possibly involved in metastasis (218, 219). Studies on STC2 have not been performed in reptiles, while expression patterns have been assessed in avian muscle and joint development (220). Roles for posttranslational deimination of STC2 remain to be understood both in reptile physiology as well as in relation to human pathologies.

Glyceraldehyde-3-phosphate dehydrogenase (GAPDH) was here identified as deiminated in alligator plasma EVs only. GAPDH is important in glycolysis, where it has key metabolic functions, while it also has pleiotropic non-metabolic functions including in mitochondrial regulation in apoptosis, in axonal transport, and in transcription activation (221-224). Furthermore, a range of moonlighting functions has been identified for GAPDH, including roles in iron metabolism (225), while it is also associated to various pathologies (223). In crocodilians, GAPDH has been studied in the muscle of caiman (226). GAPDH has been shown to be regulated via some posttranslational modifications (224, 227, 228) and was recently identified as a deimination candidate by our group in cancer (61), as well as in whales (75) and to form part of deiminated protein EV cargo in naked mole rat plasma (79). Deimination of GAPDH may contribute to its multifaceted physiological functions, and the identification of its deimination in several taxa with unusual metabolism and cancer resistance is of considerable interest.

Desmoplakin was found deiminated in alligator plasma EVs only in the current study. It is an important component of desmosomal cell-cell junctions and also involved in the coordination of cell migration as well as in maintaining integrity of the cytoskeletal intermediate filament network (229). In the *Xenopus laevis* embryo, it is required for morphogenesis and for epidermal integrity (230). A range of allergies have been

linked to mutations in desmoplakin, as well as metabolic wasting (SAM) syndrome and severe dermatitis (231). Desmoplakin has also roles in Carvajal syndrome, relating to hair abnormalities and altered skin (232). It is furthermore related to heart diseases, including cardiomyopathies (233), and found to interact with desmin, which is related to cardiomyopathies (234, 235). Other roles for desmosomal proteins relate to both tumorsuppressive and tumor-promoting functions, which depends on the type of cancer, and they can furthermore regulate cell migration, differentiation, proliferation, and apoptosis, as well as impacting sensitivity to treatment in different types of cancers (236). Interestingly, desmoplakin has recently been identified in deiminated form in camelid EVs (77), therefore indicating that enrichment of deiminated desmoplakin in EVs is found across taxa. As the functions of desmosomal proteins are not fully understood in cancer or metastasis, the current identification of deimination in alligator EVs here may be of considerable interest, also due to important roles of EV-mediated communication in the preparation of the metastatic niche. This may further current understanding of the diverse functional ability of desmoplakin, via such posttranslational modification.

Heat-shock protein mitochondrial was found to be deiminated in alligator plasma EVs only. Heat-shock proteins are phylogenetically conserved chaperone proteins involved in protein folding, protein degradation, and the stabilization of proteins against heat stress (237, 238). Heat-shock proteins are involved in mitochondrial metabolic reprogramming and therefore of importance in pro- and antioncogenic pathways (239). Heat-shock proteins are also involved in inflammation, can act as damage-associated molecular patterns (DAMPs) (240), and have furthermore been identified to be deiminated in human autoimmune disease (241). Previously, some heatshock proteins have been verified as deimination candidates by our group in teleost fish, camelid, and cetaceans (56, 75, 77), as well as in plasma EVs of naked mole rat (79). Finding posttranslational deimination of heat-shock proteins throughout phylogeny supports translational investigations between species to further current understanding of their diverse physiological and pathobiological functions.

In the current study, we report for the first time deimination signatures of plasma and plasma-derived EVs of American alligator. Posttranslational deimination of major key immune and metabolic factors was identified and related to pathways ECM-receptor interaction, ribosome, adipocytokine signaling, biosynthesis of amino acids, and glycolysis/gluconeogenesis. The reported findings highlights posttranslational deimination as an important factor in protein moonlighting, including via EV-mediated transport. Our findings furthermore contribute to a growing body of research investigating posttranslational regulation of antipathogenic and anticancerous, as well as metabolic and inflammatory pathways via posttranslational deimination and EV-mediated transport of such modified proteins. EV research in comparative animal models is an understudied but recently growing field, and this is, to our knowledge, the first characterization of EVs and associated deiminated protein cargo in a reptile. As PADs have been identified as a major player in the regulation of EV release (59–61) including in host–pathogen interactions (62, 82), such PAD-mediated contributions to cell communication remain to be further investigated both in response to physiological and pathophysiological changes, as well as in zoonotic diseases.

CONCLUSION

This is the first study to assess protein deimination profiles in plasma and EVs of a non-avian reptile, using A. mississippiensis as a model organism. KEGG pathways identified to be specific to deiminated proteins in whole plasma related to adipocytokine signaling, while KEGG pathways of deiminated proteins specific to EVs included ribosome, biosynthesis of amino acids, and glycolysis/gluconeogenesis pathways, as well as core histones. This highlights roles for EVmediated export of deiminated protein cargo functioning in metabolism and gene regulation, also related to cancer. The identification of posttranslational deimination and EVmediated communication in alligator plasma revealed here contributes to current understanding of protein moonlighting functions and EV-mediated communication in these ancient reptiles, providing novel insight into their unusual immune systems and physiological traits. Comparative studies in long-lived animals with unusual immune and metabolic functions, including cancer, antiviral and antibacterial resistance, may be of translational value for furthering current understanding of mechanisms underlying such pathogenic pathways, including via the diversification of protein function by posttranslational deimination.

DATA AVAILABILITY STATEMENT

All datasets generated for this study are included in the article/Supplementary Material.

ETHICS STATEMENT

The animal study was reviewed and approved by The Texas A&M Institutional Care and Use Committee. Sample collection was conducted under Texas A&M Institutional Animal Care and Use Protocol #2015–0347.

AUTHOR CONTRIBUTIONS

MC: resources, validation, and writing—review and editing. IK: methodology, resources, visualization. LP: resources, methodology. SL: conceptualization, data curation, formal analysis, funding acquisition, investigation, methodology, project administration, resources, validation, visualization, Writing—original draft, and writing—review and editing.

FUNDING

This study was funded in part by a University of Westminster start-up grant to SL and US National Science Foundation

grant IOS 1656870 to MC. Thanks are due to The Guy Foundation for funding the purchase of equipment utilized in this work.

ACKNOWLEDGMENTS

The authors would like to thank Yagnesh Umrania and Michael Deery at the Cambridge Centre for Proteomics for the LC-MS/MS analysis.

REFERENCES

- Janke A, Arnason U. The complete mitochondrial genome of Alligator mississippiensis and the separation between recent archosauria (birds and crocodiles). Mol Biol Evol. (1997) 14:1266–72. doi:10.1093/oxfordjournals.molbev.a025736
- Kumar S, Hedges SB. A molecular timescale for vertebrate evolution. *Nature*. (1998) 392:917–20. doi: 10.1038/31927
- Wang X, Cheng G, Lu Y, Zhang C, Wu X, Han H, et al. A comprehensive analysis of the phylogeny, genomic organization and expression of immunoglobulin light chain genes in Alligator sinensis, an endangered reptile species. *PLoS ONE*. (2016) 11:e0147704. doi:10.1371/journal.pone.0147704
- Khan NA, Soopramanien M, Siddiqui R. Crocodiles and alligators: physicians' answer to cancer? Curr Oncol. (2019) 26:186. doi: 10.3747/co.26.4855
- Merchant ME, Mills K, Leger N, Jerkins E, Vliet KA, McDaniel N. Comparisons of innate immune activity of all known living crocodylian species. Comp Biochem Physiol B Biochem Mol Biol. (2006) 143:133–7. doi:10.1016/j.cbpb.2005.10.005
- Bishop BM, Juba ML, Devine MC, Barksdale SM, Rodriguez CA, Chung MC, et al. Bioprospecting the American alligator (Alligator mississippiensis) host defense peptidome. PLoS ONE. (2015) 10:e0117394. doi: 10.1371/journal.pone.0117394
- Barksdale SM, Hrifko EJ, Chung EM, van Hoek ML. Peptides from American alligator plasma are antimicrobial against multi-drug resistant bacterial pathogens including *Acinetobacter baumannii*. *BMC Microbiol*. (2016) 16:189. doi: 10.1186/s12866-016-0799-z
- Barksdale SM, Hrifko EJ, van Hoek ML. Cathelicidin antimicrobial peptide from Alligator mississippiensis has antibacterial activity against multi-drug resistant Acinetobacter baumanii and Klebsiella pneumoniae. Dev Comp Immunol. (2017) 70:135–44. doi: 10.1016/j.dci.2017.01.011
- Merchant ME, Pallansch M, Paulman RL, Wells JB, Nalca A, Ptak R. Antiviral activity of serum from the American alligator (Alligator mississippiensis). Antiviral Res. (2005) 66:35–8. doi: 10.1016/j.antiviral.2004. 12.007
- Sweazea KL, McMurtry JP, Elsey RM, Redig P, Braun EJ. Comparison of metabolic substrates in alligators and several birds of prey. *Zoology*. (2014) 117:253–60. doi: 10.1016/j.zool.2014.04.002
- Mondal S, Thompson PR. Protein arginine deiminases (PADs): biochemistry and chemical biology of protein citrullination. *Acc Chem Res.* (2019) 52:818– 32. doi: 10.1021/acs.accounts.9b00024
- Alghamdi M, Al Ghamdi KA, Khan RH, Uversky VN, Redwan EM. An interplay of structure and intrinsic disorder in the functionality of peptidylarginine deiminases, a family of key autoimmunity-related enzymes. *Cell Mol Life Sci.* (2019) 76:4635–62. doi: 10.1007/s00018-019-0 i3237 8
- Zheng L, Nagar M, Maurais AJ, Slade DJ, Parelkar SS, Coonrod SA, et al. Calcium regulates the nuclear localization of protein arginine deiminase 2. Biochemistry. (2019) 58:3042–56. doi: 10.1021/acs.biochem.9b00225
- Vossenaar ER, Zendman AJ, van Venrooij WJ, Pruijn GJ. PAD, a growing family of citrullinating enzymes: genes, features and involvement in disease. *Bioessays*. (2003) 25:1106–18. doi: 10.1002/bies.10357

SUPPLEMENTARY MATERIAL

The Supplementary Material for this article can be found online at: https://www.frontiersin.org/articles/10.3389/fimmu. 2020.00651/full#supplementary-material

Supplementary Table 1 | F95-enriched proteins from plasma of American alligator (*Alligator mississippiensis*). Full details of protein hits are reported.

Supplementary Table 2 | F95-enriched proteins from plasma-EVs of American alligator (*Alligator mississippiensis*) plasma. Full details of protein hits are reported.

- György B, Toth E, Tarcsa E, Falus A, Buzas EI. Citrullination: a posttranslational modification in health and disease. *Int J Biochem Cell Biol.* (2006) 38:1662–77. doi: 10.1016/j.biocel.2006.03.008
- Bicker KL, Thompson PR. The protein arginine deiminases: structure, function, inhibition, and disease. *Biopolymers*. (2013) 99:155–63. doi: 10.1002/bip.22127
- Wang S, Wang Y. Peptidylarginine deiminases in citrullination, gene regulation, health and pathogenesis. Biochim Biophys Acta. (2013) 1829:1126–35. doi: 10.1016/j.bbagrm.2013.07.003
- Slade DJ, Horibata S, Coonrod SA, Thompson PR. A novel role for protein arginine deiminase 4 in pluripotency: the emerging role of citrullinated histone H1 in cellular programming. *Bioessays*. (2014) 36:736– 40. doi: 10.1002/bies.201400057
- Witalison EE, Thompson PR, Hofseth LJ. Protein arginine deiminases and associated citrullination: physiological functions and diseases associated with dysregulation. Curr Drug Targets. (2015) 16:700–10. doi: 10.2174/1389450116666150202160954
- Lange S, Gallagher M, Kholia S, Kosgodage US, Hristova M, Hardy J, et al. Peptidylarginine deiminases-roles in cancer and neurodegeneration and possible avenues for therapeutic intervention via modulation of exosome and microvesicle (EMV) release? *Int J Mol Sci.* (2017) 18:E1196. doi: 10.3390/ijms18061196
- Zhai Q, Wang L, Zhao P, Li T. Role of citrullination modification catalyzed by peptidylarginine deiminase 4 in gene transcriptional regulation. *Acta Biochim Biophys Sin.* (2017) 49:567–72. doi: 10.1093/abbs/gmx042
- Yuzhalin AE. Citrullination in cancer. Cancer Res. (2019) 79:1274–84. doi: 10.1158/0008-5472.CAN-18-2797
- Henderson B and Martin AC. Protein moonlighting: a new factor in biology and medicine. Biochem Soc Trans. (2014) 42:1671–8. doi: 10.1042/BST20140273
- Jeffrey CJ. Protein moonlighting: what is it, and why is it important? *Philos Trans R Soc Lond B Biol Sci.* (2018) 373:20160523. doi: 10.1098/rstb.2016.0523
- Mohanan S, Cherrington BD, Horibata S, McElwee JL, Thompson PR, Coonrod SA. Potential role of peptidylarginine deiminase enzymes and protein citrullination in cancer pathogenesis. *Biochem Res Int.* (2012) 2012:895343. doi: 10.1155/2012/895343
- Brentville VA, Vankemmelbeke M, Metheringham RL, Durrant LG.
 Post-translational modifications such as citrullination are excellent targets for cancer therapy. Semin Immunol. (2020) 47:101393. doi: 10.1016/j.smim.2020.101393
- 27. Uysal-Onganer P, MacLatchy A, Mahmoud R, Kraev I, Thompson PR, Inal J, et al. Peptidylarginine deiminase isozyme-specific PAD2, PAD3 and PAD4 inhibitors differentially modulate extracellular vesicle signatures and cell invasion in two glioblastoma multiforme cell lines. *Int J Mol Sci.* (2020) 21:E1495. doi: 10.3390/ijms21041495
- Darrah E, Andrade F. Rheumatoid arthritis and citrullination. Curr Opin Rheumatol. (2018) 30:72–8. doi: 10.1097/BOR.000000000000452
- Tilvawala R, Nguyen SH, Maurais AJ, Nemmara VV, Nagar M, Salinger AJ, et al. The rheumatoid arthritis-associated citrullinome. *Cell Chem Biol.* (2018) 25:691–704.e6. doi: 10.1016/j.chembiol.2018.03.002
- 30. Romero V, Darrah E, Andrade F. Peptidylarginine deiminase type 2 and 4 generate distinct patterns of rheumatoid arthritis autoantigens

- during perforin-induced cell damage. *Arthritis Rheumatol.* (2019). doi: 10.1002/art.41196. [Epub ahead of print].
- Martinez-Prat L, Palterer B, Vitiello G, Parronchi P, Robinson WH, Mahler M. Autoantibodies to protein-arginine deiminase (PAD) 4 in rheumatoid arthritis: immunological and clinical significance, and potential for precision medicine. Expert Rev Clin Immunol. (2019) 15:1073–87. doi: 10.1080/1744666X.2020.1668778
- Svärd A, Renvert S, Sanmartin Berglund J, Persson RG, Söderlin M.
 Antibodies to citrullinated peptides in serum and saliva in patients with
 rheumatoid arthritis and their association to periodontitis. Clin Exp
 Rheumatol. (2019). [Epub ahead of print].
- Fert-Bober J, Darrah E, Andrade F. Insights into the study and origin of the citrullinome in rheumatoid arthritis. *Immunol Rev.* (2020) 294:133–47. doi: 10.1111/imr.12834
- Mastronardi FG, Wood DD, Mei J, Raijmakers R, Tseveleki V, Dosch HM, et al. Increased citrullination of histone H3 in multiple sclerosis brain and animal models of demyelination: a role for tumor necrosis factor-induced peptidylarginine deiminase 4 translocation. *J Neurosci.* (2006) 26:11387–96. doi: 10.1523/INEUROSCI.3349-06.2006
- Moscarello MA, Lei H, Mastronardi FG, Winer S, Tsui H, Li Z, et al. Inhibition of peptidyl-arginine deiminases reverses proteinhypercitrullination and disease in mouse models of multiple sclerosis. *Dis Model Mech.* (2013) 6:467–78. doi: 10.1242/dmm.010520
- Wei L, Wasilewski E, Chakka SK, Bello AM, Moscarello MA, Kotra LP. Novel inhibitors of protein arginine deiminase with potential activity in multiple sclerosis animal model. *J Med Chem.* (2013) 56:1715–22. doi: 10.1021/jm301755q
- Yang L, Tan D, Piao H. Myelin basic protein citrullination in multiple sclerosis: a potential therapeutic target for the pathology. *Neurochem Res.* (2016) 41:1845–56. doi: 10.1007/s11064-016-1920-2
- 38. Faigle W, Cruciani C, Wolski W, Roschitzki B, Puthenparampil M, Tomas-Ojer P, et al. Brain citrullination patterns and T cell reactivity of cerebrospinal fluid-derived CD4+ T cells in multiple sclerosis. *Front Immunol.* (2019) 10:540. doi: 10.3389/fimmu.2019.00540
- Méchin MC, Takahara H, Simon M. Deimination and peptidylarginine deiminases in skin physiology and diseases. *Int J Mol Sci.* (2020) 21:E566. doi: 10.3390/ijms21020566
- Lange S, Gögel S, Leung KY, Vernay B, Nicholas AP, Causey CP, et al. Protein deiminases: new players in the developmentally regulated loss of neural regenerative ability. *Dev Biol.* (2011) 355:205–14. doi: 10.1016/j.ydbio.2011.04.015
- 41. Lange S, Rocha-Ferreira E, Thei L, Mawjee P, Bennett K, Thompson PR, et al. Peptidylarginine deiminases: novel drug targets for prevention of neuronal damage following hypoxic ischemic insult (HI) in neonates. *J Neurochem.* (2014) 130:555–62. doi: 10.1111/jnc.12744
- Lange S. Peptidylarginine deiminases as drug targets in neonatal hypoxic-ischemic encephalopathy. Front Neurol. (2016) 7:22. doi: 10.3389/fneur.2016.00022
- Sase T, Arito M, Onodera H, Omoteyama K, Kurokawa MS, Kagami Y, et al. Hypoxia-induced production of peptidylarginine deiminases and citrullinated proteins in malignant glioma cells. *Biochem Biophys Res Commun.* (2017) 482:50–6. doi: 10.1016/j.bbrc.2016.10.154
- 44. Yu R, Li C, Sun L, Jian L, Ma Z, Zhao J, et al. Hypoxia induces production of citrullinated proteins in human fibroblast-like synoviocytes through regulating HIF1α. Scand J Immunol. (2018) 87:e12654. doi: 10.1136/annrheumdis-2018-eular.6626
- Falcão AM, Meijer M, Scaglione A, Rinwa P, Agirre E, Liang J, et al. PAD2-mediated citrullination contributes to efficient oligodendrocyte differentiation and myelination. *Cell Rep.* (2019) 27:1090–102.e10. doi: 10.1016/j.celrep.2019.03.108
- Ding D, Enriquez-Algeciras M, Bhattacharya SK, Bonilha VL. Protein deimination in aging and age-related diseases with ocular manifestations. In: Nicholas A, Bhattacharya S, Thompson P, editors. Protein Deimination in Human Health and Disease. Cham: Springer (2017). p. 241–251.
- Wong SL, Wagner DD. Peptidylarginine deiminase 4: a nuclear button triggering neutrophil extracellular traps in inflammatory diseases and aging. FASEB J. (2018) 32:fj201800691R. doi: 10.1096/fj.201800691R

- Pan B, Alam HB, Chong W, Mobley J, Liu B, Deng Q, et al. CitH3: a reliable blood biomarker for diagnosis and treatment of endotoxic shock. Sci Rep. (2017) 7:8972. doi: 10.1038/s41598-017-09337-4
- Biron BM, Chung CS, Chen Y, Wilson Z, Fallon EA, Reichner JS, et al. PAD4 deficiency leads to decreased organ dysfunction and improved survival in a dual insult model of hemorrhagic shock and sepsis. *J Immunol*. (2018) 200:1817–28. doi: 10.4049/jimmunol.1700639
- 50. Claushuis TAM, van der Donk LEH, Luitse AL, van Veen HA, van der Wel NN, van Vught LA, et al. Role of peptidylarginine deiminase 4 in neutrophil extracellular trap formation and host defense during Klebsiella pneumoniae-induced pneumonia-derived sepsis. J Immunol. (2018) 201:1241–52. doi: 10.4049/jimmunol.1800314
- 51. Costa NA, Gut AL, Azevedo PS, Polegato BF, Magalhães ES, Ishikawa LLW, et al. Peptidylarginine deiminase 4 concentration, but not PADI4 polymorphisms, is associated with ICU mortality in septic shock patients. J Cell Mol Med. (2018) 22:4732–7. doi: 10.1111/jcmm.13717
- 52. Liang Y, Pan B, Alam HB, Deng Q, Wang Y, Chen E, et al. Inhibition of peptidylarginine deiminase alleviates LPS-induced pulmonary dysfunction and improves survival in a mouse model of lethal endotoxemia. *Eur J Pharmacol.* (2018) 833:432–40. doi: 10.1016/j.ejphar.2018.07.005
- 53. Muraro SP, De Souza GF, Gallo SW, Da Silva BK, De Oliveira SD, Vinolo MAR, et al. Respiratory syncytial virus induces the classical ROS-dependent NETosis through PAD-4 and necroptosis pathways activation. *Sci Rep.* (2018) 8:14166. doi: 10.1038/s41598-018-32576-y
- 54. Stobernack T, du Teil Espina M, Mulder LM, Palma Medina LM, Piebenga DR, et al. A secreted bacterial peptidylarginine deiminase can neutralize human innate immune defenses. MBio. (2018) 9:e01704-18. doi: 10.1128/mBio.01704-18
- Saha P, Yeoh BS, Xiao X, Golonka RM, Singh V, Wang Y, et al. PAD4-dependent NETs generation are indispensable for intestinal clearance of Citrobacter rodentium. Mucosal Immunol. (2019) 12:761–71. doi: 10.1038/s41385-019-0139-3
- Magnadottir B, Hayes P, Hristova M, Bragason BT, Nicholas AP, Dodds AW, et al. Post-translational protein deimination in cod (*Gadus morhua* L.) ontogeny novel roles in tissue remodelling and mucosal immune defences? *Dev Comp Immunol*. (2018) 87:157–70. doi: 10.1016/j.dci.2018.
- Magnadottir B, Hayes P, Gísladóttir B, Bragason B, Hristova M, Nicholas AP, et al. Pentraxins CRP-I and CRP-II are post-translationally deiminated and differ in tissue specificity in cod (*Gadus morhua* L.) ontogeny. *Dev Comp Immunol.* (2018) 87:1–11. doi: 10.1016/j.dci.2018.05.014
- Magnadottir B, Bragason BT, Bricknell IR, Bowden T, Nicholas AP, Hristova M, et al. Peptidylarginine deiminase and deiminated proteins are detected throughout early halibut ontogeny complement components C3 and C4 are post-translationally deiminated in halibut (*Hippoglossus hippoglossus L.*). Dev Comp Immunol. (2019) 92:1–19. doi: 10.1016/j.dci.2018. 10.016
- Kholia S, Jorfi S, Thompson PR, Causey CP, Nicholas AP, Inal JM, et al. A novel role for peptidylarginine deiminases (PADs) in microvesicle release: a therapeutic potential for PAD inhibitors to sensitize prostate cancer cells to chemotherapy. J Extracell Vesicles. (2015) 4:26192. doi: 10.3402/jev.v4.26192
- Kosgodage US, Trindade RP, Thompson PT, Inal JM, Lange S. Chloramidine/Bisindolylmaleimide-I-mediated inhibition of exosome and microvesicle release and enhanced efficacy of cancer chemotherapy. *Int* J Mol Sci. (2017) 18:E1007. doi: 10.3390/ijms18051007
- 61. Kosgodage US, Onganer PU, Maclatchy A, Nicholas AP, Inal JM, Lange, S. Peptidylarginine deiminases post-translationally deiminate prohibitin and modulate extracellular vesicle release and miRNAs 21 and 126 in glioblastoma multiforme. *Int J Mol Sci.* (2018) 20:E103. doi: 10.3390/ijms20010103
- Kosgodage US, Matewele P, Mastroianni G, Kraev I, Brotherton D, Awamaria B, et al. Peptidylarginine deiminase inhibitors reduce bacterial membrane vesicle release and sensitize bacteria to antibiotic treatment. Front Cell Infect Microbiol. (2019) 9:227. doi: 10.3389/fcimb.2019.00227
- Inal JM, Ansa-Addo EA, Lange S. Interplay of host-pathogen microvesicles and their role in infectious disease. *Biochem Soc Trans*. (2013) 41:258–62. doi: 10.1042/BST20120257

- Colombo M, Raposo G, Théry C. Biogenesis, secretion, and intercellular interactions of exosomes and other extracellular vesicles. *Annu Rev Cell Dev Biol.* (2014) 30:255–89. doi: 10.1146/annurev-cellbio-101512-122326
- Turchinovich A, Drapkina O, Tonevitsky A. Transcriptome of extracellular vesicles: state-of-the-art. Front Immunol. (2019) 10:202. doi: 10.3389/fimmu.2019.00202
- Vagner T, Chin A, Mariscal J, Bannykh S, Engman DM, Di Vizio D. Protein composition reflects extracellular vesicle heterogeneity. *Proteomics*. (2019) 19:e1800167. doi: 10.1002/pmic.201800167
- Hessvik NP, Llorente A. Current knowledge on exosome biogenesis and release. Cell Mol Life Sci. (2018) 75:193–208. doi: 10.1007/s00018-017-2595-9
- Ramirez SH, Andrews AM, Paul D, Pachter JS. Extracellular vesicles: mediators and biomarkers of pathology along CNS barriers. *Fluids Barriers CNS*. (2018) 15:19. doi: 10.1186/s12987-018-0104-7
- Iliev D, Strandskog G, Nepal A, Aspar A, Olsen R, Jørgensen J, et al. Stimulation of exosome release by extracellular DNA is conserved across multiple cell types. FEBS J. (2018) 285:3114–33. doi: 10.1111/febs. 14601
- Gatien J, Mermillod P, Tsikis G, Bernardi O, Janati Idrissi S, Uzbekov R, et al. Metabolomic profile of oviductal extracellular vesicles across the estrous cycle in cattle. *Int J Mol Sci.* (2019) 20:6339. doi: 10.3390/ijms20 246339
- 71. Montaner-Tarbes S, Pujol M, Jabbar T, Hawes P, Chapman D, Portillo HD, et al. Serum-derived extracellular vesicles from African swine fever virus-infected pigs selectively recruit viral and porcine proteins. *Viruses*. (2019) 11:E882. doi: 10.3390/v11100882
- Šimundić M, Švara T, Štukelj R, Krek JL, Gombač M, Kralj-Iglič V, et al. Concentration of extracellular vesicles isolated from blood relative to the clinical pathological status of dogs with mast cell tumours. *Vet Comp Oncol.* (2019) 17:456–64. doi: 10.1111/vco.12489
- Magnadottir B, Kraev I, Guð*mundsdóttir S, Dodds AW, Lange S. Extracellular vesicles from cod (*Gadus morhua* L.) mucus contain innate immune factors and deiminated protein cargo. *Dev Comp Immunol*. (2019) 99:103397. doi: 10.1016/j.dci.2019.103397
- Magnadottir B, Uysal-Onganer P, Kraev I, Dodds AW, Gudmundsdottir S, Lange S. Extracellular vesicles, deiminated protein cargo and microRNAs are novel serum biomarkers for environmental rearing temperature in Atlantic cod (Gadus morhua L.). Aquacult Rep. (2020) 16:100245. doi: 10.1016/j.aqrep.2019.100245
- Magnadottir B, Uysal-Onganer P, Kraev I, Svansson V, Hayes P, Lange S. Deiminated proteins and extracellular vesicles - novel serum biomarkers in whales and orca. Comp Biochem Physiol Part D Genomics Proteomics. (2020) 34:100676. doi: 10.1016/i.cbd.2020.100676
- Criscitiello MF, Kraev I, Lange S. Deiminated proteins in extracellular vesicles and plasma of nurse shark (*Ginglymostoma cirratum*) - novel insights into shark immunity. *Fish Shellfish Immunol.* (2019) 92:249–55. doi: 10.1016/j.fsi.2019.06.012
- Criscitiello MF, Kraev I, Lange S. Deiminated proteins in extracellular vesicles and serum of llama (Lama glama)-novel insights into camelid immunity. Mol Immunol. (2020) 117:37–53. doi: 10.1016/j.molimm.2019.10.017
- Lange S, Kraev I, Magnadóttir B, Dodds AW. Complement component C4-like protein in Atlantic cod (*Gadus morhua* L.) - detection in ontogeny and identification of post-translational deimination in serum and extracellular vesicles. *Dev Comp Immunol*. (2019) 101:103437. doi: 10.1016/j.dci.2019.103437
- Pamenter ME, Uysal-Onganer P, Huynh KW, Kraev I, Lange S. Posttranslational deimination of immunological and metabolic protein markers in plasma and extracellular vesicles of naked mole-Rat (*Heterocephalus glaber*). *Int J Mol Sci.* (2019) 20:E5378. doi: 10.3390/ijms20215378
- Phillips RA, Kraev I, Lange S. Protein deimination and extracellular vesicle profiles in Antarctic seabirds. *Biology*. (2020) 9:E15. doi: 10.3390/biology9010015
- 81. Rebl A, Köllner B, Anders E, Wimmers K, Goldammer T. Peptidylarginine deiminase gene is differentially expressed in freshwater and

- brackish water rainbow trout. *Mol Biol Rep.* (2010) 37:2333-9. doi: 10.1007/s11033-009-9738-5
- Gavinho B, Rossi IV, Evans-Osses I, Lange S, Ramirez MI. Peptidylarginine deiminase inhibition abolishes the production of large extracellular vesicles from *Giardia intestinalis*, affecting host-pathogen interactions by hindering adhesion to host cells. *bioRxiv*. (2019) 586438. doi: 10.1101/586438
- El-Sayed ASA, Shindia AA, AbouZaid AA, Yassin AM, Ali GS, Sitohy MZ. Biochemical characterization of peptidylarginine deiminase-like orthologs from thermotolerant *Emericella dentata* and *Aspergillus nidulans*. *Enzyme Microb Technol*. (2019) 124:41–53. doi: 10.1016/j.enzmictec.2019.02.004
- 84. Bielecka E, Scavenius C, Kantyka T, Jusko M, Mizgalska D, Szmigielski B, et al. Peptidyl arginine deiminase from *Porphyromonas gingivalis* abolishes anaphylatoxin C5a activity. *J Biol Chem.* (2014) 289:32481–7. doi: 10.1074/jbc.C114.617142
- Hamilton MT, Kupar CA, Kelley MD, Finger JWJr, Tuberville TD. Blood and plasma biochemistry reference intervals for wild juvenile American alligators (Alligator mississippiensis). J Wildl Dis. (2016) 52:631–5. doi: 10.7589/2015-10-275
- 86. Hamilton MT, Finger JWJr, Elsey RM, Mastromonaco GF, Tuberville TD. Corticosterone in American alligator (Alligator mississippiensis) tail scutes: evaluating the feasibility of using unconventional samples for investigating environmental stressors. Gen Comp Endocrinol. (2018) 268:7–13. doi: 10.1016/j.ygcen.2018.07.008
- 87. Finger JW Jr., Hamilton MT, Kelley MD, Stacy NI, Glenn TC, Tuberville TD. Examining the effects of chronic selenium exposure on traditionally used stress parameters in juvenile american alligators (Alligator mississippiensis). Arch Environ Contam Toxicol. (2019) 77:14–21. doi: 10.1007/s00244-019-00626-9
- 88. Faulkner PC, Hala D, Rahman MS, Petersen LH. Short-term exposure to 12‰ brackish water has significant effects on the endocrine physiology of juvenile American alligator (Alligator mississippiensis). Comp Biochem Physiol A Mol Integr Physiol. (2019) 236:110531. doi: 10.1016/j.cbpa.2019.110531
- Théry C, Witwer KW, Aikawa E, Alcaraz MJ, Anderson JD, Andriantsitohaina R, et al. Minimal information for studies of extracellular vesicles 2018 (MISEV2018): a position statement of the International Society for Extracellular Vesicles and update of the MISEV2014 guidelines. *J Extracell Vesicles*. (2018) 7:1535750. doi: 10.1080/20013078.2018.1535750
- Nicholas AP, Whitaker JN. Preparation of a monoclonal antibody to citrullinated epitopes: its characterization and some applications to immunohistochemistry in human brain. Glia. (2002) 37:328–36. doi: 10.1002/glia.10039
- Kosgodage US, Matewele P, Awamaria B, Kraev I, Warde P, Mastroianni G, et al. Cannabidiol is a novel modulator of bacterial membrane vesicles. Front Cell Infect Microbiol. (2019) 9:324. doi: 10.3389/fcimb.2019.00324
- 92. Mitchell A, Chang HY, Daugherty L, Fraser M, Hunter S, Lopez R. The interpro protein families database: the classification resource after 15 years. *Nucleic Acids Res.* (2015) 43:D213–21. doi: 10.1093/nar/gku1243
- 93. Darrah E, Rosen A, Giles JT, Andrade F. Peptidylarginine deiminase 2, 3 and 4 have distinct specificities against cellular substrates: novel insights into autoantigen selection in rheumatoid arthritis. *Ann Rheum Dis.* (2012) 71:92–8. doi: 10.1136/ard.2011.151712
- Kozlowski HN, Lai ET, Havugimana PC, White C, Emili A, Sakac D, et al. Extracellular histones identified in crocodile blood inhibit in-vitro HIV-1 infection. AIDS. (2016) 30:2043–52. doi: 10.1097/QAD.0000000000 001159
- Brinkmann V, Reichard U, Goosmann C, Fauler B, Uhlemann Y, Weiss DS, et al. Neutrophil extracellular traps kill bacteria. *Science*. (2004) 303:1532–5. doi: 10.1126/science.1092385
- Katkar GD, Sundaram MS, NaveenKumar SK, Swethakumar B, Sharma RD, Paul M, et al. NETosis and lack of DNase activity are key factors in *Echis carinatus* venom-induced tissue destruction. *Nat Commun.* (2016) 7:11361. doi: 10.1038/ncomms11361
- 97. Swethakumar B, NaveenKumar SK, Katkar GD, Girish KS, Kemparaju K. Inhibition of *Echis carinatus* venom by DNA, a promising therapeutic molecule for snakebite management. *Biochim Biophys Acta Gen Subj.* (2018) 1862:1115–25. doi: 10.1016/j.bbagen.2018.02.003

- Konig MF, Andrade F. A critical reappraisal of neutrophil extracellular traps and NETosis mimics based on differential requirements for protein citrullination. Front Immunol. (2016) 7:461. doi: 10.3389/fimmu.2016.00461
- Bao Y, Wang L, Shi L, Yun F, Liu X, Chen Y, et al. Transcriptome profiling revealed multiple genes and ECM-receptor interaction pathways that may be associated with breast cancer. *Cell Mol Biol Lett.* (2019) 24:38. doi: 10.1186/s11658-019-0162-0
- Mardpour S, Hamidieh AA, Taleahmad S, Sharifzad F, Taghikhani A, Baharvand H. Interaction between mesenchymal stromal cell-derived extracellular vesicles and immune cells by distinct protein content. *J Cell Physiol.* (2019) 234:8249–58. doi: 10.1002/jcp.27669
- Jarvis ED, Mirarab S, Aberer AJ, Li B, Houde P, Li C, et al. Whole-genome analyses resolve early branches in the tree of life of modern birds. *Science*. (2014) 346:1320–31. doi: 10.1126/science.1253451
- Yamauchi T, Kamon J, Ito Y, Tsuchida A, Yokomizo T, Kita S, et al. Cloning of adiponectin receptors that mediate antidiabetic metabolic effects. *Nature*. (2003) 423:762–9. doi: 10.1038/nature01705
- 103. Frankenberg ADV, Reis AF, Gerchman F. Relationships between adiponectin levels, the metabolic syndrome, and type 2 diabetes: a literature review. Arch Endocrinol Metab. (2017) 61:614–22. doi: 10.1590/2359-3997000000316
- 104. Yamauchi T, Kamon J, Minokoshi Y, Ito Y, Waki H, Uchida S, et al. Adiponectin stimulates glucose utilization and fatty-acid oxidation by activating AMP-activated protein kinase. Nat Med. (2002) 8:1288–95. doi: 10.1038/nm788
- Kadowaki T, Yamauchi T. Adiponectin and adiponectin receptors. *Endocr Rev.* (2005) 26:439–51. doi: 10.1210/er.2005-0005
- 106. Almabouada F, Diaz-Ruiz A, Rabanal-Ruiz Y, Peinado JR, Vazquez-Martinez R, Malagon MM. Adiponectin receptors form homomers and heteromers exhibiting distinct ligand binding and intracellular signaling properties. *J Biol Chem.* (2013) 288:3112–25. doi: 10.1074/jbc.M112.404624
- 107. Fiaschi T, Magherini F, Gamberi T, Modesti PA, Modesti A. Adiponectin as a tissue regenerating hormone: more than a metabolic function. *Cell Mol Life* Sci. (2014) 71:1917–25. doi: 10.1007/s00018-013-1537-4
- 108. Chen YL, Tao J, Zhao PJ, Tang W, Xu JP, Zhang KQ, et al. Adiponectin receptor PAQR-2 signaling senses low temperature to promote C. elegans longevity by regulating autophagy. Nat Commun. (2019) 10:2602. doi: 10.1038/s41467-019-10475-8
- 109. Parida S, Siddharth S, Sharma D. Adiponectin, obesity, and cancer: clash of the bigwigs in health and disease. *Int J Mol Sci.* (2019) 20:2519. doi: 10.3390/ijms20102519
- Gamberi T, Magherini F, Fiaschi T. Adiponectin in myopathies. *Int J Mol Sci.* (2019) 20:E1544. doi: 10.3390/ijms20071544
- 111. Chen L, Zhang YH, Lu G, Huang T, Cai YD. Analysis of cancer-related lncRNAs using gene ontology and KEGG pathways. Artif Intell Med. (2017) 76:27–36. doi: 10.1016/j.artmed.2017.02.001
- Fry B, Carter JF. Stable carbon isotope diagnostics of mammalian metabolism, a high-resolution isotomics approach using amino acid carboxyl groups. PLoS ONE. (2019) 14:e0224297. doi: 10.1371/journal.pone.0224297
- 113. Merchant ME, Roche C, Elsey RM, Prudhomme J. Antibacterial properties of serum from the American alligator (*Alligator mississippiensis*). Comp Biochem Physiol B Biochem Mol Biol. (2003) 136:505–13. doi: 10.1016/S1096-4959(03)00256-2
- Merchant M, Thibodeaux D, Loubser K, Elsey RM. Amoebacidal effects of serum from the American alligator (Alligator mississippiensis). J Parasitol. (2004) 90:1480–3. doi: 10.1645/GE-3382
- Dodds AW, Law SK. The phylogeny and evolution of the thioester bondcontaining proteins C3, C4 and alpha 2-macroglobulin. *Immunol Rev.* (1998) 166:15–26. doi: 10.1111/j.1600-065X.1998.tb01249.x
- Fishelson Z, Attali G, Mevorach D. Complement and apoptosis. Mol Immunol. (2001) 38:207–19. doi: 10.1016/S0161-5890(01)00055-4
- Hart SP, Smith JR, Dransfield I. Phagocytosis of opsonized apoptotic cells: roles for 'old-fashioned' receptors for antibody and complement. Clin Exp Immunol. (2004) 135:181–5. doi: 10.1111/j.1365-2249.2003.02330.x
- Carroll MV, Sim RB. Complement in health and disease. Adv Drug Deliv Rev. (2011) 63:965–75. doi: 10.1016/j.addr.2011.06.005
- Morgan BP, Walters D, Serna M, Bubeck D. Terminal complexes of the complement system: new structural insights and their relevance to function. *Immunol Rev.* (2016) 274:141–51. doi: 10.1111/imr.12461

- Chen JY, Cortes C, Ferreira VP. Properdin: a multifaceted molecule involved in inflammation and diseases. *Mol Immunol.* (2018) 102:58–72. doi: 10.1016/j.molimm.2018.05.018
- Dobó J, Kocsis A, Gál P. Be on target: strategies of targeting alternative and lectin pathway components in complement-mediated diseases. Front Immunol. (2018) 9:1851. doi: 10.3389/fimmu.2018.01851
- 122. Harrison RA. The properdin pathway: an "alternative activation pathway" or a "critical amplification loop" for C3 and C5 activation? Semin Immunopathol. (2018) 40:15–35. doi: 10.1007/s00281-017-0661-x
- Lachmann PJ. Looking back on the alternative complement pathway. *Immunobiology*. (2018) 223:519–23. doi: 10.1016/j.imbio.2018.02.001
- Schröder-Braunstein J, Kirschfink M. Complement deficiencies and dysregulation: pathophysiological consequences, modern analysis, and clinical management. *Mol Immunol.* (2019) 114:299–311. doi: 10.1016/j.molimm.2019.08.002
- Boshra H, Li J, Sunyer JO. Recent advances on the complement system of teleost fish. Fish Shellfish Immunol. (2006) 20:239–62. doi: 10.1016/j.fsi.2005.04.004
- 126. Sunyer JO, Lambris JD. Evolution and diversity of the complement system of poikilothermic vertebrates. *Immunol Rev.* (1998) 166:39–57. doi:10.1111/j.1600-065X.1998.tb01251.x
- 127. Nakao M, Kato-Unoki Y, Nakahara M, Mutsuro J, Somamoto T. Diversified components of the bony fish complement system: more genes for robuster innate defense? Adv Exp Med Biol. (2006) 586:121–38. doi: 10.1007/0-387-34134-X 9
- Nakao M, Tsujikura M, Ichiki S, Vo TK, Somamoto T. The complement system in teleost fish: progress of post-homolog-hunting researches. *Dev Comp Immunol*. (2011) 35:1296–308. doi: 10.1016/j.dci.2011.03.003
- 129. Forn-Cuní G, Reis ES, Dios S, Posada D, Lambris JD, Figueras A, et al. The evolution and appearance of C3 duplications in fish originate an exclusive teleost c3 gene form with anti-inflammatory activity. *PLoS ONE*. (2014) 9:e99673. doi: 10.1371/journal.pone.0099673
- Kommanee J, Preecharram S, Daduang S, Temsiripong Y, Dhiravisit A, Yamada Y, et al. Antibacterial activity of plasma from crocodile (*Crocodylus siamensis*) against pathogenic bacteria. *Ann Clin Microbiol Antimicrob*. (2012) 11:22. doi: 10.1186/1476-0711-11-22
- 131. Phosri S, Mahakunakorn P, Lueangsakulthai J, Jangpromma N, Swatsitang P, Daduang S, et al. An investigation of antioxidant and anti-inflammatory activities from blood components of Crocodile (*Crocodylus siamensis*). Protein J. (2014) 33:484–92. doi: 10.1007/s10930-014-9581-y
- 132. Lu J, Teh C, Kishore U, Reid KB. Collectins and ficolins: sugar pattern recognition molecules of the mammalian innate immune system. *Biochim Biophys Acta*. (2002) 1572:387–400. doi: 10.1016/S0304-4165(02) 00320-3
- 133. García-Laorden MI, Hernández-Brito E, Muñoz-Almagro C, Pavlovic-Nesic S, Rúa-Figueroa I, Briones ML, et al. Should MASP-2 deficiency be considered a primary immunodeficiency? Relevance of the lectin pathway. J Clin Immunol. (2019) 40:203–10. doi: 10.1007/s10875-019-00714-4
- 134. Barkai LJ, Sipter E, Csuka D, Prohászka Z, Pilely K, Garred P, et al. Decreased ficolin-3-mediated complement lectin pathway activation and alternative pathway amplification during ibacterial infections in patients with type 2 diabetes mellitus. Front Immunol. (2019) 10:509. doi: 10.3389/fimmu.2019.00509
- Dadfar E, Furuhjelm C, Nilsson J, Dahle C, Garred P. Fatal pneumococcus meningitis in a child with complement factor ficolin-3 deficiency. J Allergy Clin Immunol Pract. (2019) 8:778–9. doi: 10.1016/j.jaip.2019.07.039
- 136. Kjældgaard AL, Pilely K, Olsen KS, Pedersen SW, Lauritsen AØ, Møller K, et al. Amyotrophic lateral sclerosis: the complement and inflammatory hypothesis. *Mol Immunol*. (2018) 102:14–25. doi: 10.1016/j.molimm.2018.06.007
- Troldborg A, Steffensen R, Trendelenburg M, Hauser T, Winther KG, Hansen AG, et al. Ficolin-3 deficiency is associated with disease and an increased risk of systemic lupus erythematosus. *J Clin Immunol*. (2019) 39:421–9. doi: 10.1007/s10875-019-00627-2
- Tizzot MR, Lidani KCF, Andrade FA, Mendes HW, Beltrame MH, Reiche E, et al. Ficolin-1 and ficolin-3 plasma levels are altered in HIV and HIV/HCV coinfected patients from Southern Brazil. Front Immunol. (2018) 9:2292. doi: 10.3389/fimmu.2018.02292

- 139. Lorenzo-Almorós A, Hang T, Peiró C, Soriano-Guillén L, Egido J, Tuñón J, et al. Predictive and diagnostic biomarkers for gestational diabetes and its associated metabolic and cardiovascular diseases. *Cardiovasc Diabetol.* (2019) 18:140. doi: 10.1186/s12933-019-0935-9
- 140. Liu X, Wang G. The effect of high-intensity interval training on physical parameters, metabolomic indexes and serum ficolin-3 levels in patients with prediabetes and type 2 diabetes. *Exp Clin Endocrinol Diabetes*. (2020) doi: 10.1055/a-1027-6511. [Epub ahead of print].
- 141. Troldborg A, Thiel S, Mistegaard CE, Hansen A, Korsholm TL, Stengaard-Pedersen K, et al. Plasma levels of H- and L-ficolin are increased in axial spondyloarthritis: improvement of disease identification. Clin Exp Immunol. (2020) 199:79–87. doi: 10.1111/cei.13374
- 142. Li Q, Lin Y. Evaluation of ficolin-3 as a potential prognostic serum biomarker in Chinese patients with esophageal cancer. *Genet Test Mol Biomark*. (2019) 23:565–72. doi: 10.1089/gtmb.2019.0045
- 143. OmPraba G, Chapeaurouge A, Doley R, Devi KR, Padmanaban P, Venkatraman C, et al. Identification of a novel family of snake venom proteins Veficolins from *Cerberus rynchops* using a venom gland transcriptomics and proteomics approach. *J Proteome Res.* (2010) 9:1882–93. doi: 10.1021/pr901044x
- 144. Hargreaves AD, Swain MT, Logan DW, Mulley JF. Testing the *Toxicofera*: comparative transcriptomics casts doubt on the single, early evolution of the reptile venom system. *Toxicon*. (2014) 92:140–56. doi: 10.1016/j.toxicon.2014.10.004
- Perales J, Neves-Ferreira AG, Valente RH, Domont GB. Natural inhibitors of snake venom hemorrhagic metalloproteinases. *Toxicon*. (2005) 45:1013–20. doi: 10.1016/j.toxicon.2005.02.028
- 146. Armstrong PB, Quigley JP. Alpha2-macroglobulin: an evolutionarily conserved arm of the innate immune system. *Dev Comp Immunol.* (1999) 23:375–90. doi: 10.1016/S0145-305X(99)00018-X
- 147. Davies SG, Sim RB. Intramolecular general acid catalysis in the binding reactions of alpha 2-macroglobulin and complement components C3 and C4. Biosci Rep. (1981) 1:461–8. doi: 10.1007/BF01121579
- 148. Sottrup-Jensen L, Stepanik TM, Kristensen T, Lønblad PB, Jones CM, Wierzbicki DM, et al. Common evolutionary origin of alpha 2-macroglobulin and complement components C3 and C4. Proc Natl Acad Sci USA. (1985) 82:9–13. doi: 10.1073/pnas.82.1.9
- Ikai A, Kitamoto T, Nishigai M. Alpha-2-macroglobulin-like protease inhibitor from the egg white of cuban crocodile (*Crocodylus rhombifer*). J Biochem. (1983) 93:121–7. doi: 10.1093/oxfordjournals.jbchem.a134145
- 150. Ikai A, Kikuchi M, Nishigai M. Internal structure of ovomacroglobulin studied by electron microscopy. *J Biol Chem.* (1990) 265:8280–4.
- 151. Nishigai M, Osada T, Ikai A. Structural changes in alpha-2- and ovomacroglobulins studied by gel chromatography and electron microscopy. Biochim Biophys Acta. (1985) 831:236–41. doi: 10.1016/0167-4838(85)90040-8
- 152. Arakawa H, Osada T, Ikai A. Unusual properties of crocodilian ovomacroglobulin shown in its methylamine treatment and sulfhydryl titration. *Arch Biochem Biophys.* (1986) 244:447–53. doi: 10.1016/0003-9861(86)90612-0
- 153. Biedzka-Sarek M, Metso J, Kateifides A, Meri T, Jokiranta TS, Muszynski A, et al. Apolipoprotein A-I exerts bactericidal activity against Yersinia enterocolitica serotype O:3. J Biol Chem. (2011) 286:38211-9. doi: 10.1074/jbc.M111.249482
- 154. Sigel S, Bunk S, Meergans T, Doninger B, Stich K, Stulnig T, et al. Apolipoprotein B100 is a suppressor of *Staphylococcus aureus*-induced innate immune responses in humans and mice. *Eur J Immunol.* (2012) 42:2983–9. doi: 10.1002/eji.201242564
- 155. Johnston LD, Brown G, Gauthier D, Reece K, Kator H, Van Veld P. Apolipoprotein A-I from striped bass (Morone saxatilis) demonstrates antibacterial activity in vitro. Comp Biochem Physiol B Biochem Mol Biol. (2008) 151:167–75. doi: 10.1016/j.cbpb.2008.06.011
- 156. Wang CQ, Yang CS, Yang Y, Pan F, He LY, Wang AM. An apolipoprotein E mimetic peptide with activities against multidrug-resistant bacteria and immunomodulatory effects. J Pept Sci. (2013) 19:745–50. doi: 10.1002/psc.2570
- 157. Ghimire D, Rai M, Gaur R. Novel host restriction factors implicated in HIV-1 replication. *J Gen Virol.* (2018) 99:435–46. doi: 10.1099/jgv.0.001026

- Van Helden P, Strickland WN, Brandt WF, Von Holt C. Histone H2B variants from the erythrocytes of an amphibian, a reptile and a bird. *Biochim Biophys Acta*. (1978) 533:278–81. doi: 10.1016/0005-2795(78)90572-X
- Svinarchuk FP, Rozov SM, Berdnikov VA. [Histone H1 of reptiles, homologous to histone H5 of birds]. Mol Biol. (1982) 16:703–11.
- 160. Krivoruchko A, Storey KB. Epigenetics in anoxia tolerance: a role for histone deacetylases. Mol Cell Biochem. (2010) 342:151–61. doi: 10.1007/s11010-010-0479-5
- 161. Wijenayake S, Hawkins LJ, Storey KB. Dynamic regulation of six histone H3 lysine (K) methyltransferases in response to prolonged anoxia exposure in a freshwater turtle. *Gene.* (2018) 649:50–7. doi: 10.1016/j.gene.2018.01.086
- 162. Holt WV. Exploitation of non-mammalian model organisms in epigenetic research. Adv Exp Med Biol. (2017) 1014:155–73. doi: 10.1007/978-3-319-62414-3_9
- 163. Siddiqui R, Jeyamogan S, Ali SM, Abbas F, Sagathevan KA, Khan NA. Crocodiles and alligators: antiamoebic and antitumor compounds of crocodiles. Exp Parasitol. (2017) 183:194–200. doi: 10.1016/j.exppara.2017.09.008
- Davis TA, Loos B, Engelbrecht AM. AHNAK: the giant jack of all trades. Cell Signal. (2014) 26:2683–93. doi: 10.1016/j.cellsig.2014.08.017
- 165. Silva TA, Smuczek B, Valadão IC, Dzik LM, Iglesia RP, Cruz MC, et al. AHNAK enables mammary carcinoma cells to produce extracellular vesicles that increase neighboring fibroblast cell motility. *Oncotarget.* (2016) 7:49998–50016. doi: 10.18632/oncotarget.10307
- 166. Witzke KE, Großerueschkamp F, Jütte H, Horn M, Roghmann F, von Landenberg N, et al. Integrated fourier transform infrared imaging and proteomics for identification of a candidate histochemical biomarker in bladder cancer. Am J Pathol. (2019) 189:619–31. doi: 10.1016/j.ajpath.2018.11.018
- 167. Li M, Liu Y, Meng Y, Zhu Y. AHNAK nucleoprotein 2 performs a promoting role in the proliferation and migration of uveal melanoma cells. *Cancer Biother Radiopharm*. (2019) 34:626–33. doi: 10.1089/cbr.2019.2778
- 168. Klett H, Fuellgraf H, Levit-Zerdoun E, Hussung S, Kowar S, Küsters S, et al. Identification and validation of a diagnostic and prognostic multi-gene biomarker panel for pancreatic ductal adenocarcinoma. Front Genet. (2018) 9:108. doi: 10.3389/fgene.2018.00108
- 169. Zhou YY, Kang YT, Chen C, Xu FF, Wang HN, Jin R. Combination of TNM staging and pathway based risk score models in patients with gastric cancer. J Cell Biochem. (2018) 119:3608–17. doi: 10.1002/jcb. 26562
- 170. Ohmura H, Ito M, Uchino K, Okada C, Tanishima S, Yamada Y, et al. Methylation of drug resistance-related genes in chemotherapy-sensitive Epstein-Barr virus-associated gastric cancer. FEBS Open Bio. (2020) 10:147– 57. doi: 10.1002/2211-5463.12765
- Kirov A, Kacer D, Conley BA, Vary CP, Prudovsky I. AHNAK2 Participates in the stress-induced nonclassical FGF1 secretion pathway. *J Cell Biochem*. (2015) 116:1522–31. doi: 10.1002/jcb.25047
- 172. Tey S, Shahrizaila N, Drew AP, Samulong S, Goh KJ, Battaloglu E, et al. Linkage analysis and whole exome sequencing reveals AHNAK2 as a novel genetic cause for autosomal recessive CMT in a Malaysian family. Neurogenetics. (2019) 20:117–27. doi: 10.1007/s10048-019-00576-3
- Wang P. Andrenomedullin and cardiovascular responses in sepsis. Peptides. (2001) 22:1835–40. doi: 10.1016/S0196-9781(01)00534-4
- 174. Fowler DE, Yang S, Zhou M, Chaudry IH, Simms HH, Wang P. Adrenomedullin and adrenomedullin binding protein-1: their role in the septic response. *J Surg Res.* (2003) 109:175–81. doi: 10.1016/S0022-4804(02)00086-0
- 175. Cheng G, Gao Y, Wang T, Sun Y, Wei Z, Li L, et al. Extensive diversification of IgH subclass-encoding genes and IgM subclass switching in crocodilians. Nat Commun. (2013) 4:1337. doi: 10.1038/ncomms2317
- Magadan-Mompo S, Sanchez-Espinel C, Gambon-Deza F. IgH loci of American alligator and saltwater crocodile shed light on IgA evolution. Immunogenetics. (2013) 65:531–41. doi: 10.1007/s00251-013-0692-y
- 177. Hutchinson D, Clarke A, Heesom K, Murphy D, Eggleton P. Carbamylation/citrullination of IgG Fc in bronchiectasis, established RA with bronchiectasis and RA smokers: a potential risk factor for disease. ERJ Open Res. (2017) 3:00018-2017. doi: 10.1183/23120541.000 18-2017

- 178. Lundqvist ML, Middleton DL, Radford C, Warr GW, Magor KE. Immunoglobulins of the non-galliform birds: antibody expression and repertoire in the duck. *Dev Comp Immunol.* (2006) 30:93–100. doi: 10.1016/j.dci.2005.06.019
- 179. de los Rios M, Criscitiello MF, Smider VV. Structural and genetic diversity in antibody repertoires from diverse species. *Curr Opin Struct Biol.* (2015) 33:27–41. doi: 10.1016/j.sbi.2015.06.002
- 180. Xu Z, Takizawa F, Parra D, Gómez D, von Gersdorff Jørgensen L, LaPatra SE, et al. Mucosal immunoglobulins at respiratory surfaces mark an ancient association that predates the emergence of tetrapods. *Nat Commun.* (2016) 7:10728. doi: 10.1038/ncomms10728
- Akula S, Hellman L. The appearance and diversification of receptors for IgM during vertebrate Evolution. Curr Top Microbiol Immunol. (2017) 408:1–23. doi: 10.1007/82 2017 22
- 182. Zhang X, Calvert RA, Sutton BJ, Doré KA. IgY: a key isotype in antibody evolution. Biol Rev Camb Philos Soc. (2017) 92:2144–56. doi: 10.1111/brv.12325
- 183. Magadan S, Krasnov A, Hadi-Saljoqi S, Afanasyev S, Mondot S, Lallias D, et al. Standardized IMGT® nomenclature of salmonidae IGH genes, the paradigm of Atlantic salmon and rainbow trout: from genomics to repertoires. Front Immunol. (2019) 10:2541. doi: 10.3389/fimmu.2019.02541
- 184. Ueda Y, Sato M. Cell membrane dynamics induction using optogenetic tools. Biochem Biophys Res Commun. (2018) 506:387–93. doi:10.1016/j.bbrc.2017.11.091
- 185. Peotter JL, Phillips J, Tong T, Dimeo K, Gonzalez JMJr, Peters DM. Involvement of Tiam1, RhoG and ELMO2/ILK in Rac1-mediated phagocytosis in human trabecular meshwork cells. Exp Cell Res. (2016) 347:301–11. doi: 10.1016/j.yexcr.2016.08.009
- 186. Boehm M, Krause-Gruszczynska M, Rohde M, Tegtmeyer N, Takahashi S, Oyarzabal OA, et al. Major host factors involved in epithelial cell invasion of *Campylobacter jejuni*: role of fibronectin, integrin beta1, FAK, Tiam-1, and DOCK180 in activating Rho GTPase Rac1. Front Cell Infect Microbiol. (2011) 1:17. doi: 10.3389/fcimb.2011.00017
- 187. Blanco-Suárez E, Fiuza M, Liu X, Chakkarapani E, Hanley JG. Differential Tiam1/Rac1 activation in hippocampal and cortical neurons mediates differential spine shrinkage in response to oxygen/glucose deprivation. J Cereb Blood Flow Metab. (2014) 34:1898–906. doi: 10.1038/jcbfm.2014.158
- 188. Veluthakal R, Kumar B, Mohammad G, Kowluru A, Kowluru RA. Tiam1-Rac1 axis promotes activation of p38 MAP Kinase in the development of diabetic retinopathy: evidence for a requisite role for protein palmitoylation. Cell Physiol Biochem. (2015) 36:208–20. doi: 10.1159/000374065
- 189. Kowluru RA, Kowluru A, Veluthakal R, Mohammad G, Syed I, Santos JM, et al. TIAM1-RAC1 signalling axis-mediated activation of NADPH oxidase-2 initiates mitochondrial damage in the development of diabetic retinopathy. *Diabetologia*. (2014) 57:1047–56. doi: 10.1007/s00125-014-3194-z
- Subramanian N, Navaneethakrishnan S, Biswas J, Kanwar RK, Kanwar JR, Krishnakumar S. RNAi mediated Tiam1 gene knockdown inhibits invasion of retinoblastoma. *PLoS ONE*. (2013) 8:e70422. doi: 10.1371/journal.pone.0070422
- Izumi D, Toden S, Ureta E, Ishimoto T, Baba H, Goel A. TIAM1 promotes chemoresistance and tumor invasiveness in colorectal cancer. *Cell Death Dis*. (2019) 10:267. doi: 10.1038/s41419-019-1493-5
- Ding J, Yang F, Wu W. Tiam1 high expression is associated with poor prognosis in solid cancers: a meta-analysis. *Medicine*. (2019) 98:e17529. doi: 10.1097/MD.000000000017529
- 193. Zhang Y, Huang J, Li Q, Chen K, Liang Y, Zhan Z, et al. Histone methyltransferase SETDB1 promotes cells proliferation and migration by interacting with Tiam1 in hepatocellular carcinoma. BMC Cancer. (2018) 18:539. doi: 10.1186/s12885-018-4464-9
- 194. Sanmartín E, Yáñez Y, Fornés-Ferrer V, Zugaza JL, Cañete A, Castel V, et al. TIAM1 variants improve clinical outcome in neuroblastoma. *Oncotarget*. (2017) 8:45286–97. doi: 10.18632/oncotarget.16787
- 195. Kurdi AT, Bassil R, Olah M, Wu C, Xiao S, Taga M, et al. Tiam1/Rac1 complex controls Il17a transcription and autoimmunity. *Nat Commun.* (2016) 7:13048. doi: 10.1038/ncomms13048
- 196. Veluthakal R, Sidarala V, Kowluru A. NSC23766, a Known Inhibitor of Tiam1-Rac1 signaling module, prevents the onset of type 1 diabetes

- in the NOD mouse model. Cell Physiol Biochem. (2016) 39:760-7. doi: 10.1159/000445666
- Kowluru A. Tiam1/Vav2-Rac1 axis: a tug-of-war between islet function and dysfunction. *Biochem Pharmacol*. (2017) 132:9–17. doi:10.1016/j.bcp.2017.02.007
- 198. Ahmed MM, Dhanasekaran AR, Tong S, Wiseman FK, Fisher EM, Tybulewicz VL, et al. Protein profiles in Tc1 mice implicate novel pathway perturbations in the down syndrome brain. *Hum Mol Genet.* (2013) 22:1709– 24. doi: 10.1093/hmg/ddt017
- 199. Wuyts W, Spieker N, Van Roy N, De Boulle K, De Paepe A, Willems PJ, et al. Refined physical mapping and genomic structure of the EXTL1 gene. Cytogenet Cell Genet. (2000) 86:267–70. doi: 10.1159/000015317
- 200. Kim BT, Kitagawa H, Tamura J, Saito T, Kusche-Gullberg M, Lindahl U, et al. Human tumor suppressor EXT gene family members EXTL1 and EXTL3 encode α1,4- N-acetylglucosaminyltransferases that likely are involved in heparan sulfate/ heparin biosynthesis. *Proc Natl Acad Sci USA*. (2001) 98:7176–81. doi: 10.1073/pnas.131188498
- 201. Stopschinski BE, Holmes BB, Miller GM, Manon VA, Vaquer-Alicea J, Prueitt WL, et al. Specific glycosaminoglycan chain length and sulfation patterns are required for cell uptake of tau versus α-synuclein and β-amyloid aggregates. *J Biol Chem.* (2018) 293:10826–40. doi: 10.1074/jbc.RA117.000378
- Mostert V. Selenoprotein P: properties, functions, and regulation. Arch Biochem Biophys. (2000) 376:433–8. doi: 10.1006/abbi.2000.1735
- Burk RF, Hill KE. Selenoprotein P-expression, functions, and roles in mammals. Biochim Biophys Acta. (2009) 1790:1441-7. doi: 10.1016/j.bbagen.2009.03.026
- Lobanov AV, Hatfield DL, Gladyshev VN. Reduced reliance on the trace element selenium during evolution of mammals. *Genome Biol.* (2008) 9:r62. doi: 10.1186/gb-2008-9-3-r62
- 205. Sutija M, Joss JM. Thyroid hormone deiodinases revisited: insights from lungfish: a review. J Comp Physiol B. (2006) 176:87–92. doi:10.1007/s00360-005-0018-y
- 206. Gunderson MP, Pickett MA, Martin JT, Hulse EJ, Smith SS, Smith LA, et al. Variations in hepatic biomarkers in American alligators (Alligator mississippiensis) from three sites in Florida, USA. Chemosphere. (2016) 155:180–7. doi: 10.1016/j.chemosphere.2016.04.018
- Urbanska K, Orzechowski A. Unappreciated role of LDHA and LDHB to control apoptosis and autophagy in tumor cells. *Int J Mol Sci.* (2019) 20:E2085. doi: 10.3390/ijms20092085
- Feichtinger RG, Lang R. Targeting L-lactate metabolism to overcome resistance to immune therapy of melanoma and other tumor entities. *J Oncol.* (2019) 2019;2084195. doi: 10.1155/2019/2084195
- 209. Chang AC, Hook J, Lemckert FA, McDonald MM, Nguyen MA, Hardeman EC, et al. The murine stanniocalcin 2 gene is a negative regulator of postnatal growth. *Endocrinology*. (2008) 149:2403–10. doi: 10.1210/en.2007-1219
- 210. Sarapio E, De Souza SK, Model JFA, Trapp M, Da Silva RSM. Stanniocalcin-1 and—2 effects on glucose and lipid metabolism in white adipose tissue from fed and fasted rats. *Can J Physiol Pharmacol.* (2019) 97:916–23. doi: 10.1139/cjpp-2019-0023
- 211. Sarapio E, De Souza SK, Vogt EL, Rocha DS, Fabres RB, Trapp M, et al. Effects of stanniocalcin hormones on rat brown adipose tissue metabolism under fed and fasted conditions. *Mol Cell Endocrinol.* (2019) 485:81–7. doi: 10.1016/j.mce.2019.02.004
- 212. Fujimoto M, Hwa V, Dauber A. Novel modulators of the growth hormone insulin-like growth factor axis: pregnancy-associated plasma protein-A2 and stanniocalcin-2. *J Clin Res Pediatr Endocrinol*. (2017) 9:1–8. doi: 10.4274/jcrpe.2017.S001
- 213. Luo CW, Pisarska MD, Hsueh AJ. Identification of a stanniocalcin paralog, stanniocalcin-2, in fish and the paracrine actions of stanniocalcin-2 in the mammalian ovary. *Endocrinology*. (2005) 146:469–76. doi: 10.1210/en.2004-1197
- 214. Zeiger W, Ito D, Swetlik C, Oh-hora M, Villereal ML, Thinakaran G. Stanniocalcin 2 is a negative modulator of store-operated calcium entry. *Mol Cell Biol.* (2011) 31:3710–22. doi: 10.1128/MCB.05140-11
- 215. Gagliardi AD, Kuo EY, Raulic S, Wagner GF, DiMattia GE. Human stanniocalcin-2 exhibits potent growth-suppressive properties in transgenic mice independently of growth hormone and IGFs. *Am J*

- Physiol Endocrinol Metab. (2005) 288:E92-105. doi: 10.1152/ajpendo.002 68 2004
- 216. He H, Qie S, Guo Q, Chen S, Zou C, Lu T, et al. Stanniocalcin 2 (STC2) expression promotes post-radiation survival, migration and invasion of nasopharyngeal carcinoma cells. *Cancer Manag Res.* (2019) 11:6411–24. doi: 10.2147/CMAR.S197607
- 217. Ito D, Walker JR, Thompson CS, Moroz I, Lin W, Veselits ML, et al. Characterization of stanniocalcin 2, a novel target of the mammalian unfolded protein response with cytoprotective properties. *Mol Cell Biol*. (2004) 24:9456–69. doi: 10.1128/MCB.24.21.9456-9469.2004
- 218. Jiang ST, Wang HQ, Yang TC, Wang DW, Yang LJ, Xi YQ, et al. Expression of stanniocalcin 2 in breast cancer and its clinical significance. *Curr Med Sci.* (2019) 39:978–83. doi: 10.1007/s11596-019-2131-2
- Hu L, Zha Y, Kong F, Pan Y. Prognostic value of high stanniocalcin 2 expression in solid cancers: a meta-analysis. *Medicine*. (2019) 98:e17432. doi: 10.1097/MD.0000000000017432
- Mittapalli VR, Pröls F, Huang R, Christ B, Scaal M. Avian stanniocalcin-2 is expressed in developing striated muscle and joints. *Anat Embryol.* (2006) 211:519–23. doi: 10.1007/s00429-006-0100-6
- 221. Tarze A, Deniaud A, Le Bras M, Maillier E, Molle D, Larochette N, et al. GAPDH, a novel regulator of the pro-apoptotic mitochondrial membrane permeabilization. *Oncogene*. (2007) 26:2606–20. doi: 10.1038/sj.onc. 1210074
- 222. Zala D, Hinckelmann MV, Yu H, Lyra da Cunha MM, Liot G, Cordelières FP, et al. Vesicular glycolysis provides on-board energy for fast axonal transport. Cell. (2013) 152:479–91. doi: 10.1016/j.cell.2012.12.029
- 223. Sirover MA. Pleiotropic effects of moonlighting glyceraldehyde-3-phosphate dehydrogenase (GAPDH) in cancer progression, invasiveness, and metastases. Cancer Metastasis Rev. (2018) 37:665–76. doi: 10.1007/s10555-018-9764-7
- 224. Butera G, Mullappilly N, Masetto F, Palmieri M, Scupoli MT, Pacchiana R, et al. Regulation of autophagy by nuclear GAPDH and its aggregates in cancer and neurodegenerative disorders. *Int J Mol Sci.* (2019) 20:E2062. doi: 10.3390/ijms20092062
- Boradia VM, Raje M, Raje CI. Protein moonlighting in iron metabolism: glyceraldehyde-3-phosphate dehydrogenase (GAPDH). *Biochem Soc Trans*. (2014) 42:1796–801. doi: 10.1042/BST20140220
- 226. Vieira MM, Veiga LA, Nakano M. Muscle D-glyceraldehyde-3-phosphate dehydrogenase from *Caiman* sp. II New data for enzyme characterization. *Comp Biochem Physiol B.* (1984) 79:427–33. doi: 10.1016/0305-0491(84)90400-0
- Tristan C, Shahani N, Sedlak TW, Sawa A. The diverse functions of GAPDH: views from different subcellular compartments. *Cell Signal*. (2011) 23:317– 23. doi: 10.1016/j.cellsig.2010.08.003
- 228. White MR, Garcin ED. D-Glyceraldehyde-3-phosphate dehydrogenase structure and function. *Subcell Biochem.* (2017) 83:413–53. doi: 10.1007/978-3-319-46503-6_15
- 229. Bendrick JL, Eldredge LA, Williams EI, Haight NB, Dubash AD. Desmoplakin harnesses Rho GTPase and p38 mitogen-activated protein kinase sSignaling to coordinate cellular migration. *J Invest Dermatol.* (2019) 139:1227–36. doi: 10.1016/j.jid.2018.11.032

- Bharathan NK, Dickinson AJG. Desmoplakin is required for epidermal integrity and morphogenesis in the *Xenopus laevis* embryo. *Dev Biol.* (2019) 450:115–31. doi: 10.1016/j.ydbio.2019.03.010
- 231. Liang J, Li C, Zhang Z, Ni C, Yu H, Li M, et al. Severe dermatitis, multiple allergies and metabolic wasting (SAM) syndrome caused by *de novo* mutation in the DSP gene misdiagnosed as generalized pustular psoriasis and treatment of acitretin with gabapentin. *J Dermatol*. (2019) 46:622–5. doi: 10.1111/1346-8138.14925
- Yermakovich D, Sivitskaya L, Vaikhanskaya T, Danilenko N, Motuk I. Novel desmoplakin mutations in familial Carvajal syndrome. Acta Myol. (2018) 37:263-6.
- 233. Reichl K, Kreykes SE, Martin CM, Shenoy C. Desmoplakin variant-associated arrhythmogenic cardiomyopathy presenting as acute myocarditis. Circ Genom Precis Med. (2018) 11:e002373. doi: 10.1161/CIRCGEN.118.002373
- 234. Tsikitis M, Galata Z, Mavroidis M, Psarras S, Capetanaki Y. Intermediate filaments in cardiomyopathy. *Biophys Rev.* (2018) 10:1007–31. doi: 10.1007/s12551-018-0443-2
- Brodehl A, Gaertner-Rommel A, Milting H. Molecular insights into cardiomyopathies associated with desmin (DES) mutations. *Biophys Rev.* (2018) 10:983–1006. doi: 10.1007/s12551-018-0429-0
- Zhou G, Yang L, Gray A, Srivastava AK, Li C, Zhang G, et al. The role of desmosomes in carcinogenesis. Onco Targets Ther. (2017) 10:4059–63. doi: 10.2147/OTT.S136367
- 237. Buchner J. Hsp90 and Co. a holding for folding. *Trends Biochem Sci.* (1999) 24:136–41. doi: 10.1016/S0968-0004(99)01373-0
- Picard D. Heat-shock protein 90, a chaperone for folding and regulation. Cell Mol Life Sci. (2002) 59:1640–8. doi: 10.1007/PL00012491
- Avolio R, Matassa DS, Criscuolo D, Landriscina M, Esposito F. Modulation of mitochondrial metabolic reprogramming and oxidative stress to overcome chemoresistance in cancer. *Biomolecules*. (2020) 10:E135. doi: 10.3390/biom10010135
- 240. Binder RJ. Functions of heat shock proteins in pathways of the innate and adaptive immune system. *J Immunol.* (2014) 193:5765–71. doi:10.4049/jimmunol.1401417
- 241. Travers TS, Harlow L, Rosas IO, Gochuico BR, Mikuls TR, Bhattacharya SK, et al. Extensive citrullination promotes immunogenicity of HSP90 through protein unfolding and exposure of cryptic epitopes. *J Immunol*. (2016) 197:1926–36. doi: 10.4049/jimmunol.1600162

Conflict of Interest: The authors declare that the research was conducted in the absence of any commercial or financial relationships that could be construed as a potential conflict of interest.

Copyright © 2020 Criscitiello, Kraev, Petersen and Lange. This is an open-access article distributed under the terms of the Creative Commons Attribution License (CC BY). The use, distribution or reproduction in other forums is permitted, provided the original author(s) and the copyright owner(s) are credited and that the original publication in this journal is cited, in accordance with accepted academic practice. No use, distribution or reproduction is permitted which does not comply with these terms